POGGIO LAB

University of Basel

Magnetic imaging on the nanometer scale

Quantum Functionalities of Nanomagnets

Ingelheim, Germany

18.06.2025

Prof. Martino Poggio

poggiolab.unibas.ch

KANTON AARGAU

Swiss Nanoscience Institute

Swiss National Science Foundation

Schweizerische Eidgenossenschaft
Confédération suisse
Confederazione Svizzera
Confederaziun svizra

Funded by the European Union

POGGIO LAB

University of Basel

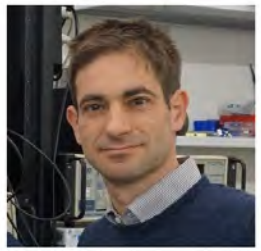

Prof. Martino Poggio
Principal Investigator

Dr. Floris Braakman
Research Scientist

Dr. Boris Gross
Research Scientist

Dr. Paritosh Karnatak
Research Scientist

Dr. Francesco Fogliano
Post-doctoral Researcher

Dr. Damien Richert
Post-doctoral Researcher

Dr. Liza Žaper
Post-doctoral Researcher

Dr. Andriani Vervelaki
Post-doctoral Researcher

Lukas Schneider
Ph.D. Student

Daniel Jetter
Ph.D. Student

Luca Forrer
Ph.D. Student

Mathias Claus
Ph.D. Student

Aurèle Kamber
Ph.D. Student

Aris Lafranca
Ph.D. Student

Antonella Restino
Ph.D. Student

Patrick Raif
Ph.D. Student

Loris Durante
Ph.D. Student

Katharina Kress
Ph.D. Student

Mirco Schwarz
Masters Student

poggiolab.unibas.ch

KANTON AARGAU

Swiss Nanoscience Institute

Swiss National Science Foundation

Schweizerische Eidgenossenschaft
Confédération suisse
Confederazione Svizzera
Confederaziun svizra

Funded by the European Union

Superconducting thin films & circuits

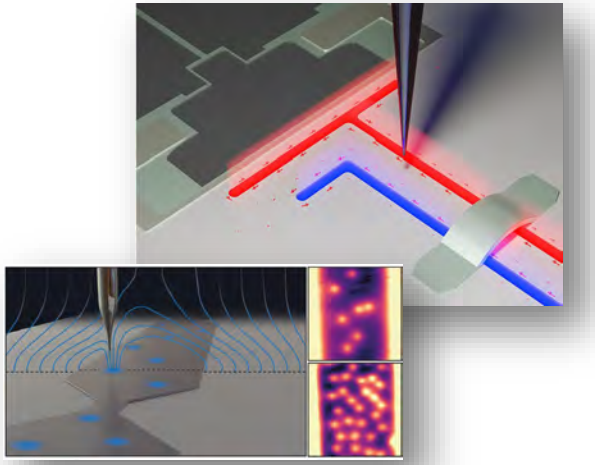

2D magnetic materials

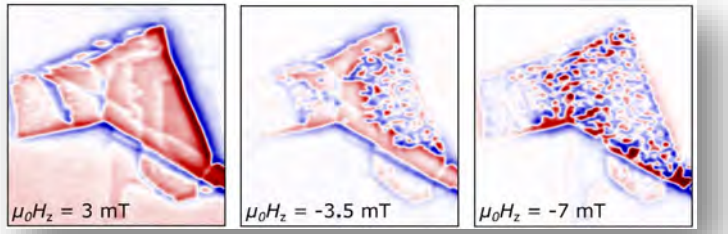

Nanomagnets

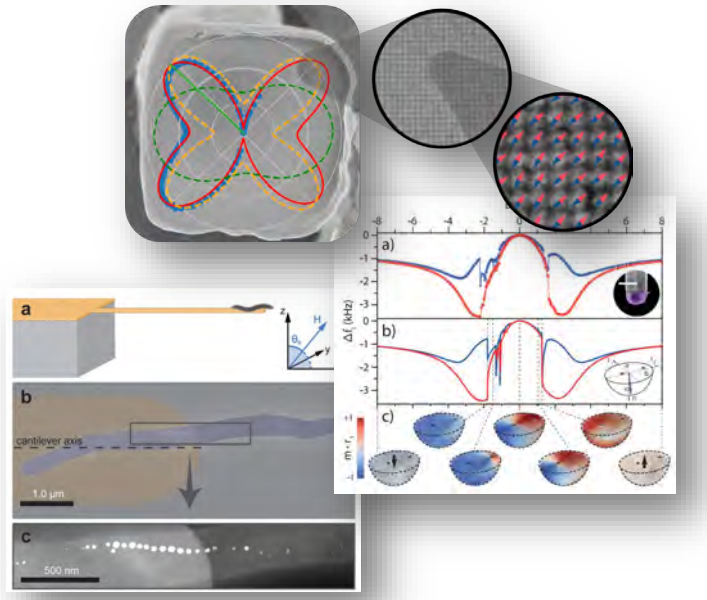

Chiral magnets

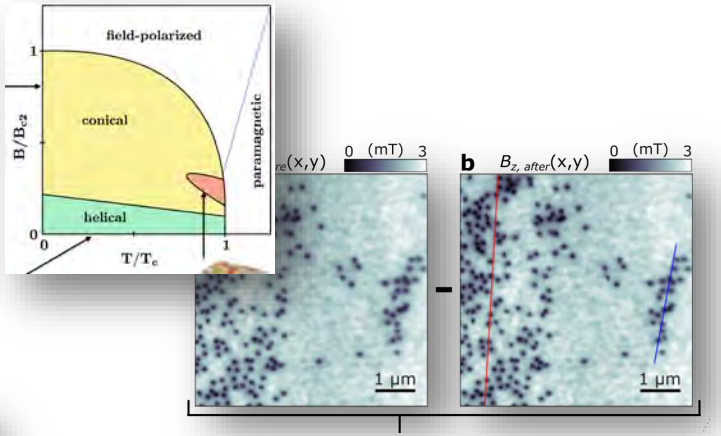

Superconducting sensors

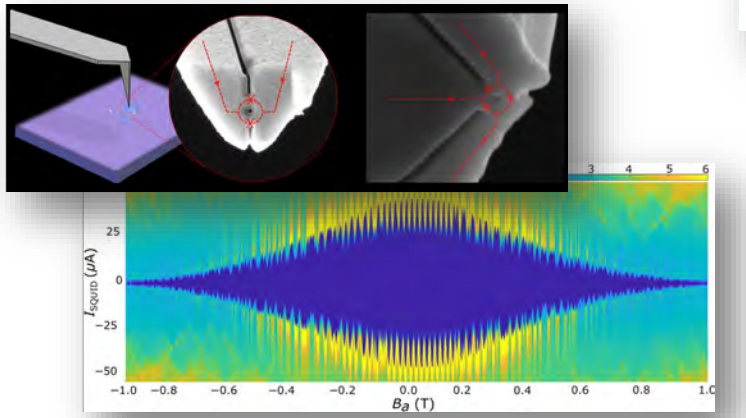

Nano & Opto-mechanics

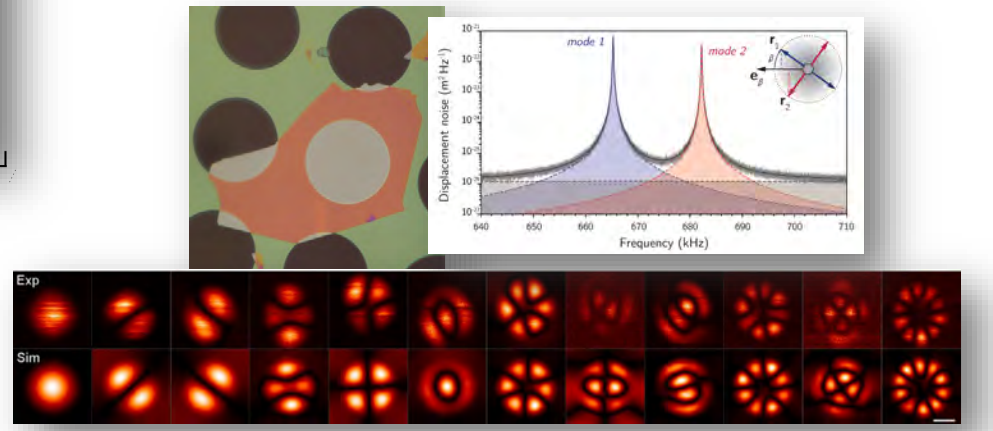

Outline

- Introduction
- Imaging magnetism via magnetic fields
- Magnetic force microscopy (MFM)
    - Bilayer $EuGe_2$
- Scanning SQUID microscopy (SSM)
    - Few-layer CrSBr
    - Monolayer CPS_4
- Conclusion

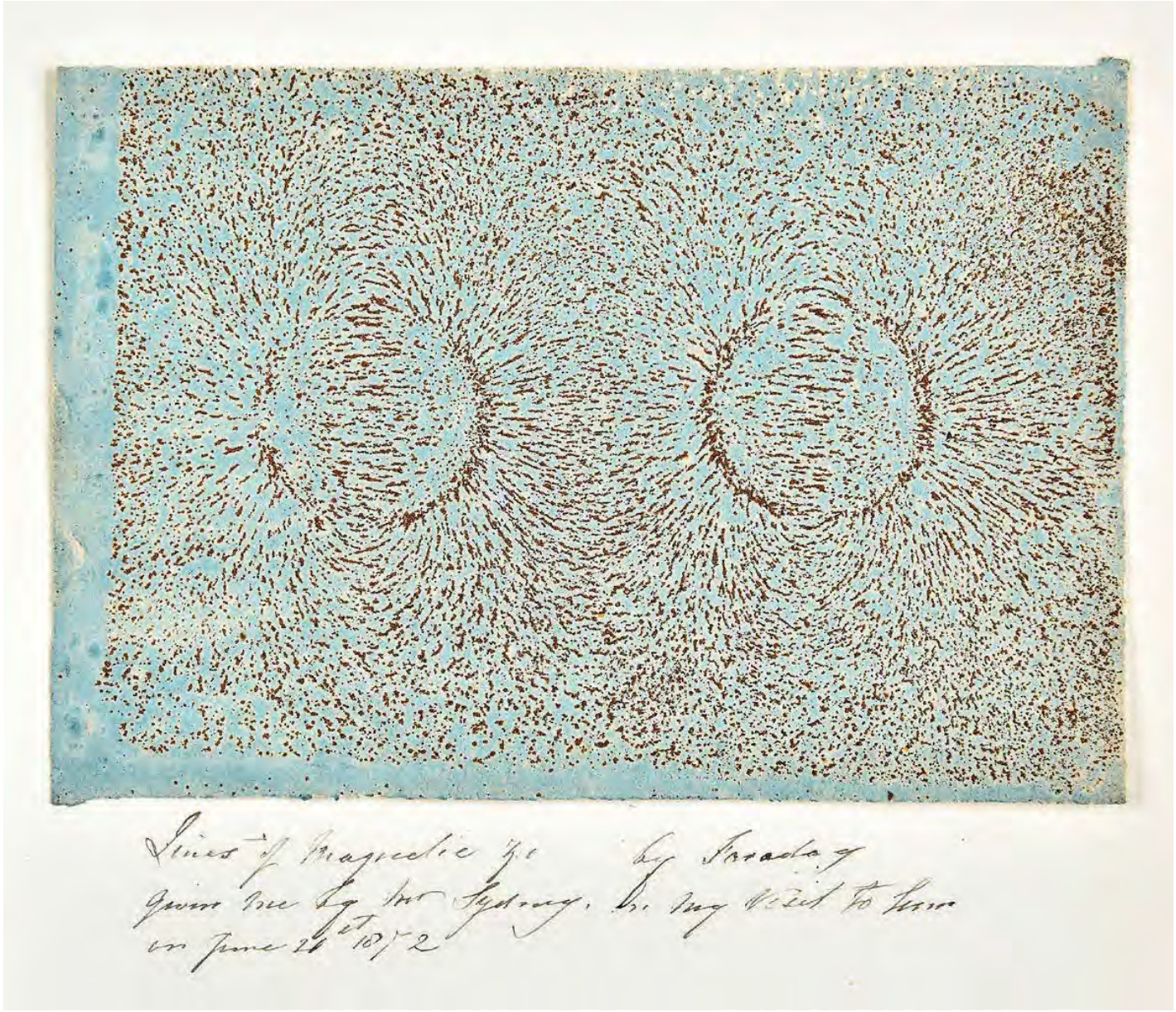

Iron filings, M. Faraday, ca. 1830s

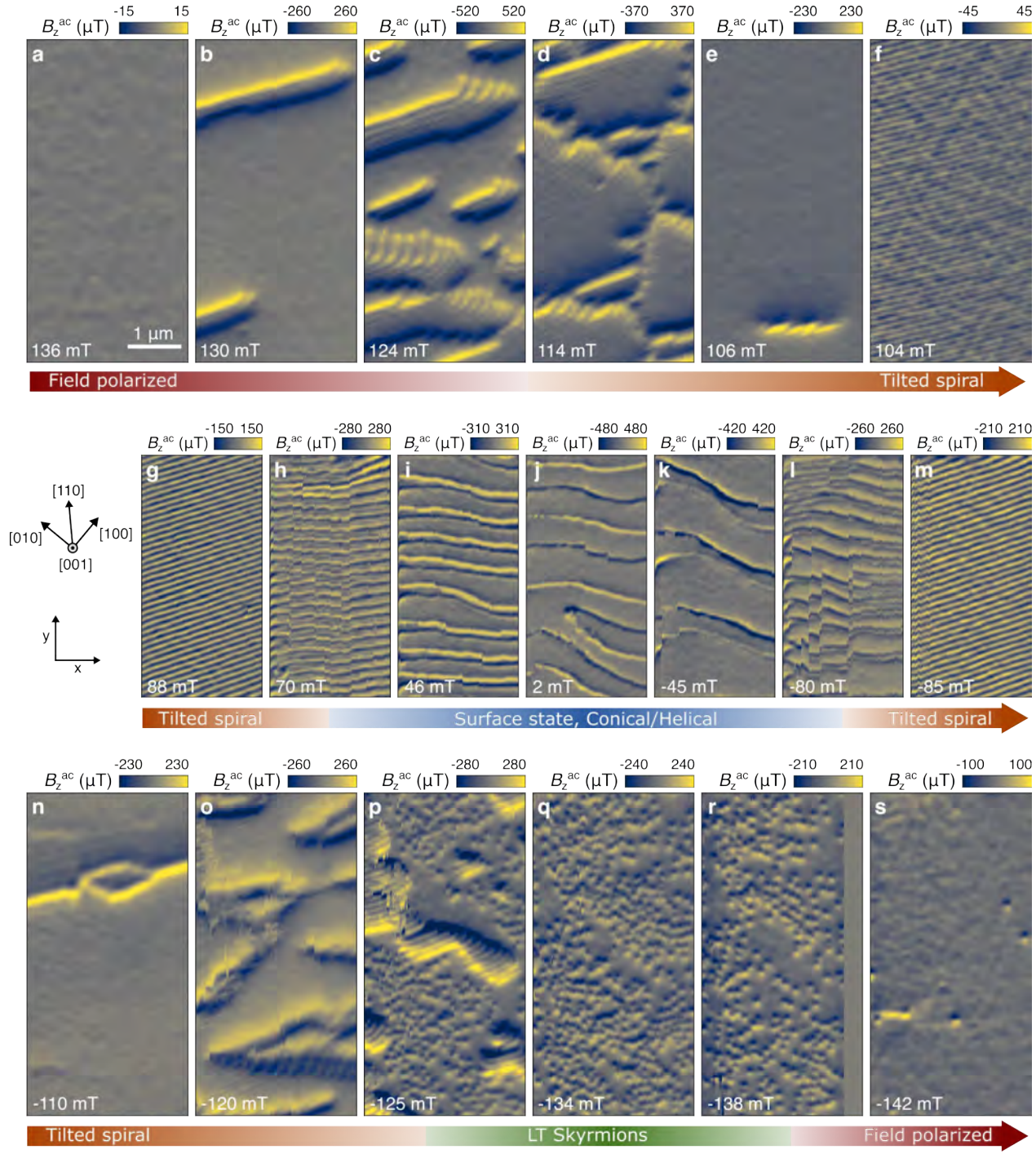

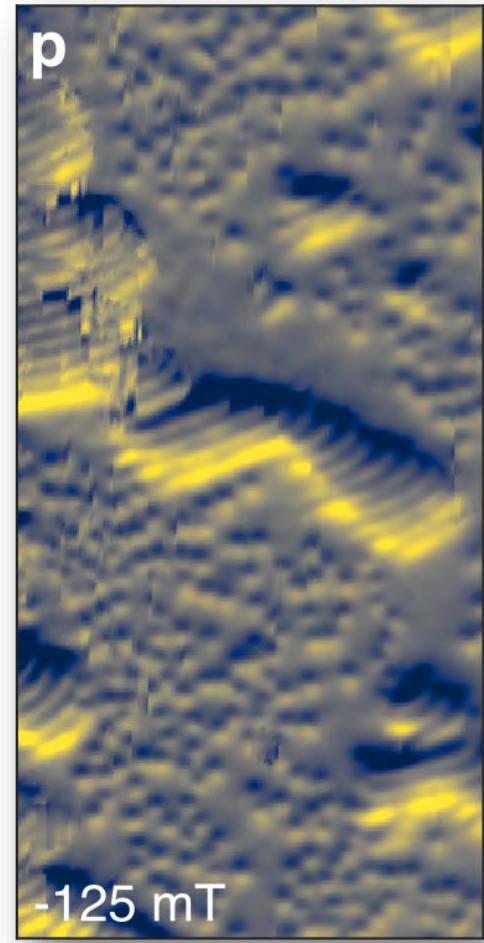

Surface of Cu_2OSeO_3, Marchiori et al.,

Commun. Mater. **5**, 202 (2024)

Energence of 2D materials and vdW heterostructures

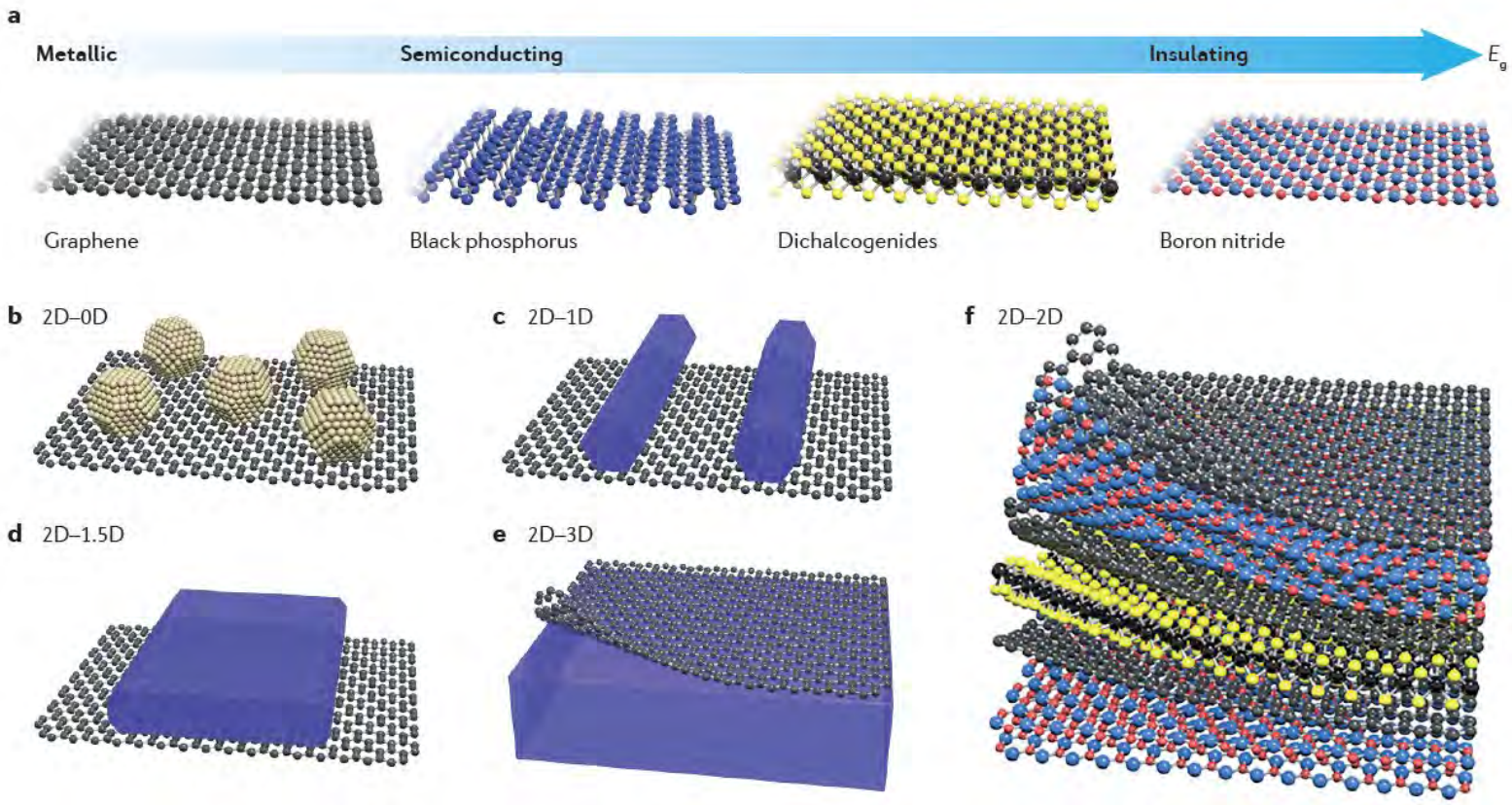

Figure 1 | **Two-dimensional layered materials and van der Waals heterostructures. a** | A broad library of two-dimensional layered materials (2DLMs) with varying chemical composition, atomic structures and electronic properties, with an increasing bandgap from left to right. **b**–**f** | Van der Waals heterostructures formed by integrating the dangling-bond-free 2DLMs with 0D nanoparticles or quantum dots (panel **b**), 1D nanowires (panel **c**), 1.5D nanoribbons (panel **d**), 3D bulk materials (panel **e**) and 2D nanosheets (panel **f**).

Liu et al., *Nat. Rev. Mater.* **1**, 1 (2016)

Energence of 2D materials and vdW heterostructures

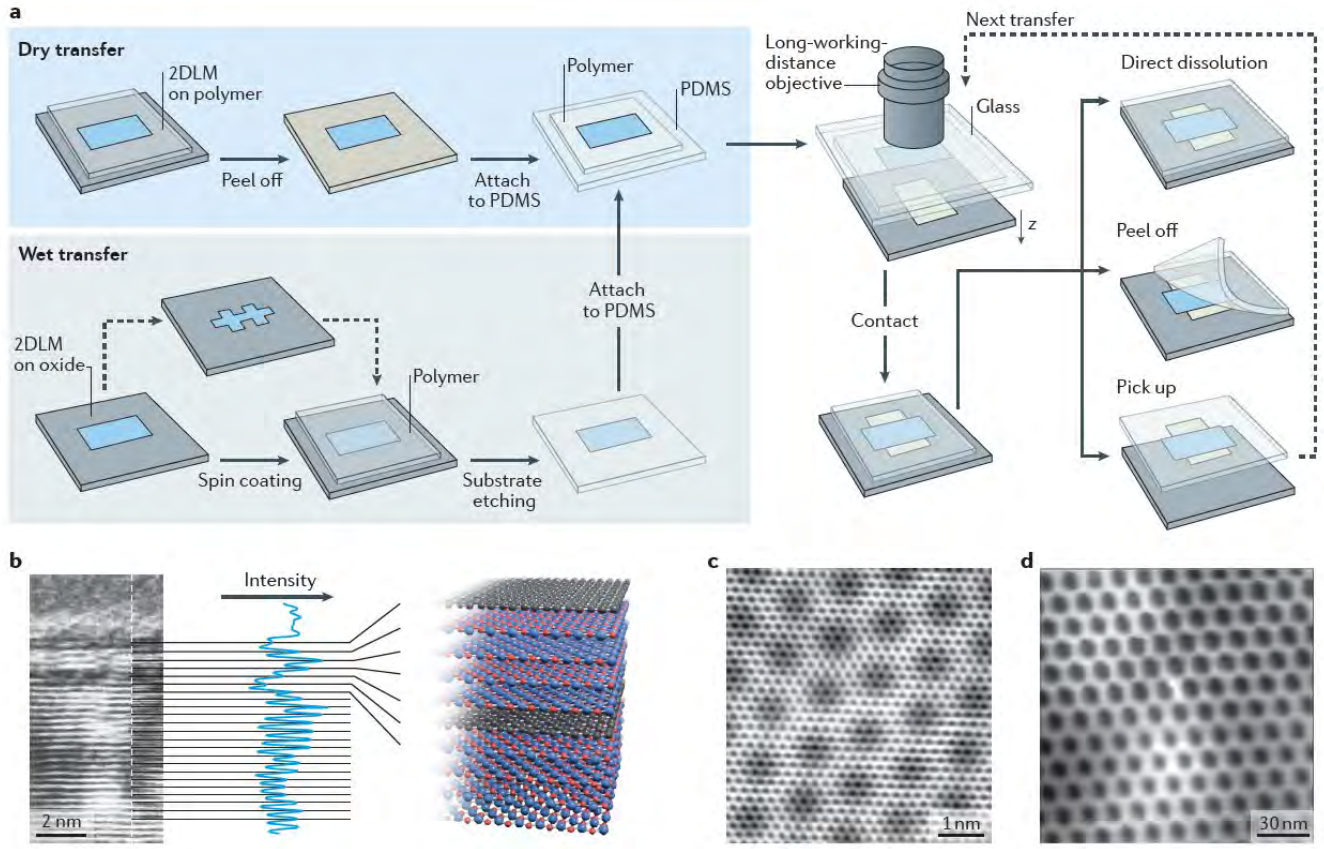

Figure 2 | **Assembly and characterization of 2D–2D vdWHs. a** | Schematic illustration of state-of-the-art alignment transfer processes for van der Waals heterostructure (vdWH) integration. Wet and dry transfer techniques are used to attach the target sheet to the stamp material. The stamp is then attached to a glass slide and placed in a transfer microscope. Micromanipulators allow for the precise alignment of sheets using a long-working-distance objective lens. The polymer transfer stamp can either be chemically dissolved away, mechanically peeled off or used to pick up the entire stack for further transfer steps. **b** | False-coloured high-resolution cross-sectional scanning tunnelling electron microscopy image of the BN–graphene–BN–graphene stack (left) and a corresponding schematic representation (right). **c**,**d** | Moiré pattern of graphene on BN (panel **c**) and a much larger moiré pattern of the commensurate–incommensurate transition of graphene on BN (panel **d**). 2DLM, two-dimensional layered material; BN, boron nitride; PDMS, poly(dimethyl siloxane). Panel **b** is from REF. 71, Nature Publishing Group. Panel **c** is courtesy of Brian LeRoy, University of Arizona, USA. Panel **d** is from REF. 73, Nature Publishing Group.

Liu et al., *Nat. Rev. Mater.* **1**, 1 (2016)

Correlated states in atomically layered materials

ARTICLE

doi:10.1038/nature26160

Unconventional superconductivity in magic-angle graphene superlattices

Yuan Cao[1], Valla Fatemi[1], Shiang Fang[2], Kenji Watanabe[3], Takashi Taniguchi[3], Efthimios Kaxiras[2,4] & Pablo Jarillo-Herrero[1]

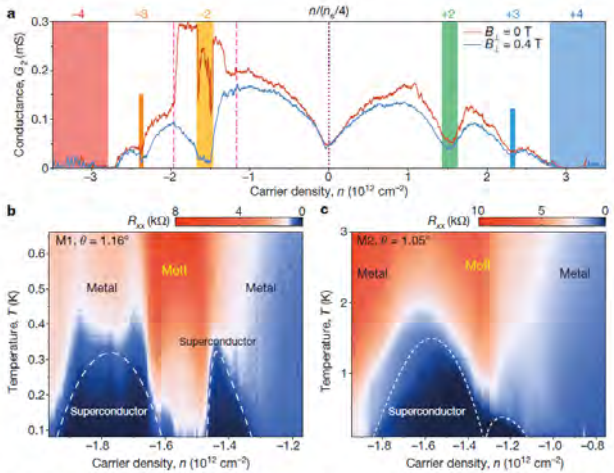

Figure 2 | Gate-tunable superconductivity in magic-angle TBG. **a**, Two-probe conductance $G_2 = I/V_{bias}$ of device M1 ($\theta = 1.16°$) measured in zero magnetic field (red) and at a perpendicular field of $B_\perp = 0.4$ T (blue). The curves exhibit the typical V-shaped conductance near charge neutrality ($n = 0$, vertical purple dotted line) and insulating states at the superlattice bandgaps $n = \pm n_s$, which correspond to filling ±4 electrons in each moiré unit cell (blue and red bars). They also exhibit reduced conductance at intermediate integer fillings of the superlattice owing to Coulomb interactions (other coloured bars). Near a filling of −2 electrons per unit cell, there is considerable conductance enhancement at zero field that is suppressed in $B_\perp = 0.4$ T. This enhancement signals the onset of superconductivity. Measurements were conducted at 70 mK; $V_{bias} = 10\,\mu$V. **b**, Four-probe resistance R_{xx}, measured at densities corresponding to the region bounded by pink dashed lines in **a**, versus temperature. Two superconducting domes are observed next to the half-filling state, which is labelled 'Mott' and centred around $-n_s/2 = -1.58 \times 10^{12}$ cm^{-2}. The remaining regions in the diagram are labelled as 'metal' owing to the metallic temperature dependence. The highest critical temperature observed in device M1 is $T_c = 0.5$ K (at 50% of the normal-state resistance). **c**, As in **b**, but for device M2, showing two asymmetric and overlapping domes. The highest critical temperature in this device is $T_c = 1.7$ K.

LETTER

doi:10.1038/nature22391

Layer-dependent ferromagnetism in a van der Waals crystal down to the monolayer limit

Bevin Huang[1]*, Genevieve Clark[2]*, Efrén Navarro-Moratalla[3]*, Dahlia R. Klein[3], Ran Cheng[4], Kyle L. Seyler[1], Ding Zhong[1], Emma Schmidgall[1], Michael A. McGuire[5], David H. Cobden[1], Wang Yao[6], Di Xiao[4], Pablo Jarillo-Herrero[3] & Xiaodong Xu[1,2]

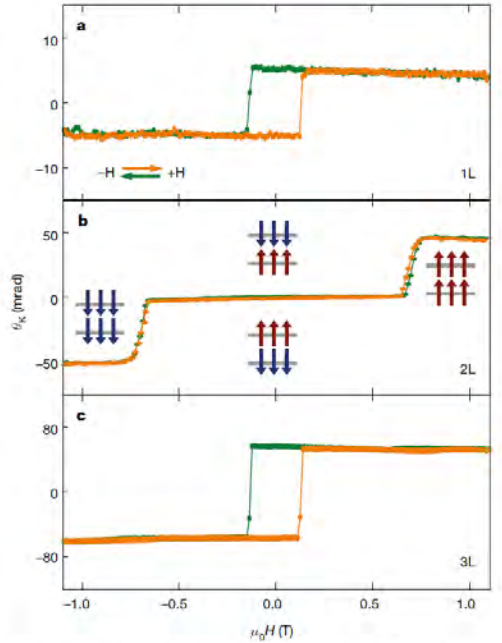

Figure 3 | Layer-dependent magnetic ordering in atomically-thin CrI_3. **a**, MOKE signal on a monolayer (1L) CrI_3 flake, showing hysteresis in the Kerr rotation as a function of applied magnetic field, indicative of ferromagnetic behaviour. **b**, MOKE signal from a bilayer CrI_3 showing vanishing Kerr rotation for applied fields ±0.65 T, suggesting antiferromagnetic behaviour. Insets depict bilayer (2L) magnetic ground states for different applied fields. **c**, MOKE signal on a trilayer (3L) flake, showing a return to ferromagnetic behaviour.

Magnetism in two-dimensions

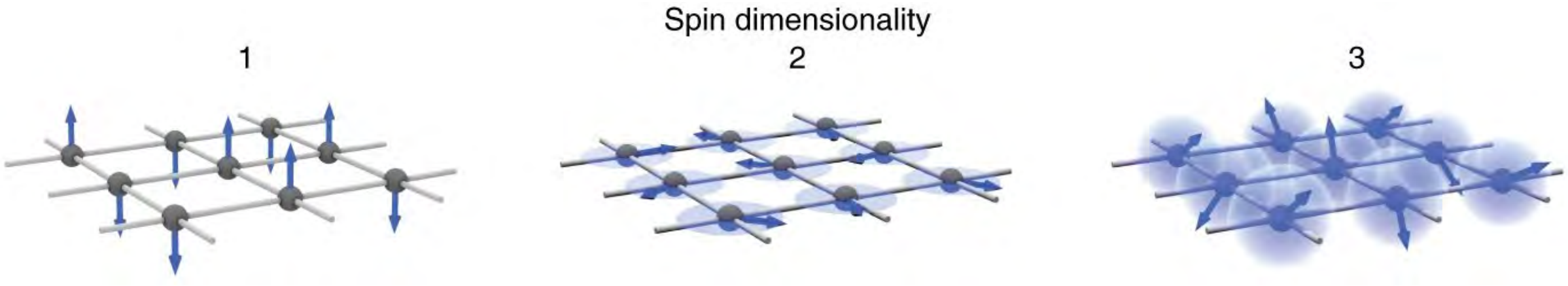

Ising

XY

Heisenberg

Model phase transitions

Unique topology

Phases governed by the Berezinski-Kosterlitz-Thouless (BKT) transition

Mermin Wagner theorem – long range order?

Existence of magnetic anisotropy becomes crucial for ordering

Nat. Nanotechnol. 14, 408–419 (2019)

Magnetic order

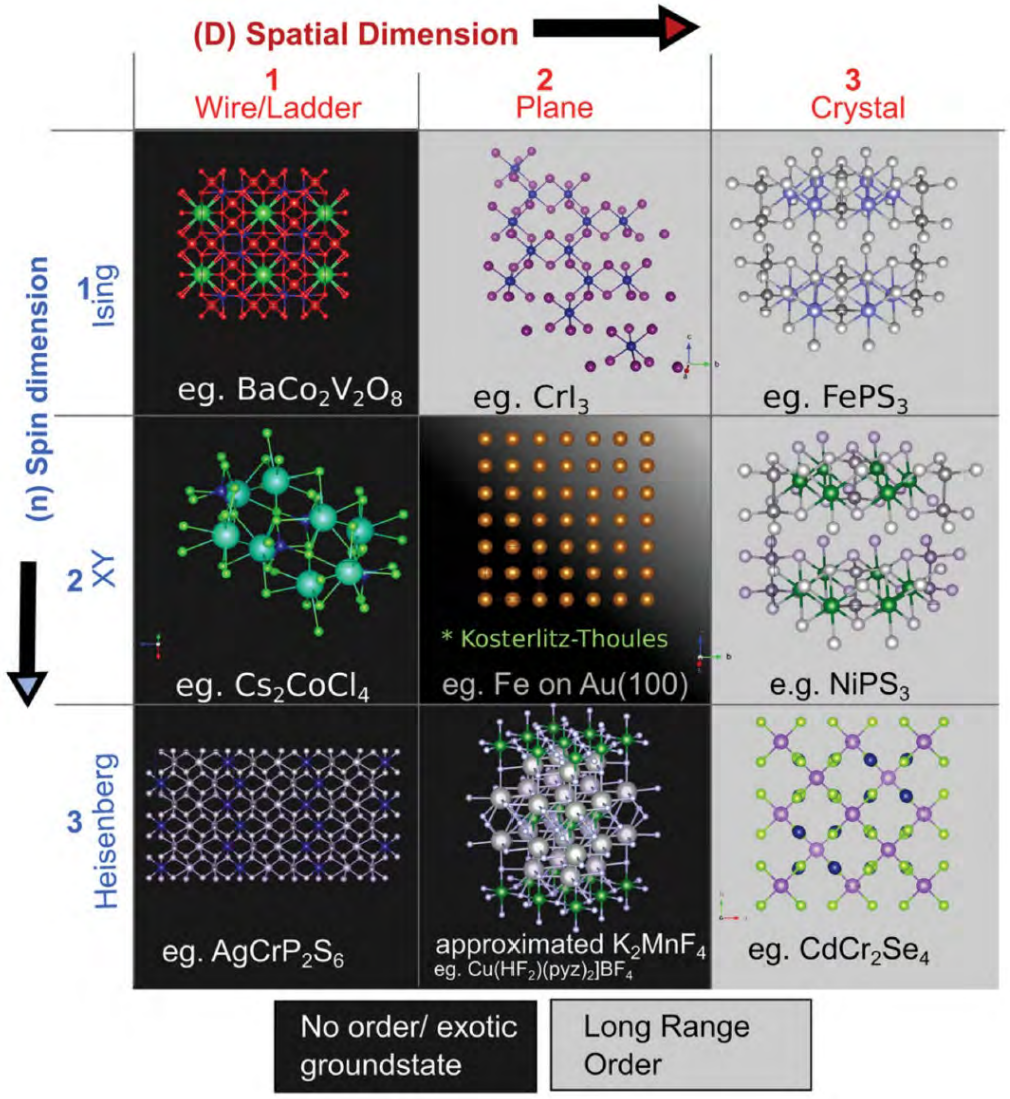

D. L. Cortie et al., *Advanced Functional Materials* **30**, 1901414 (2020).

Two-dimensional magnetism timeline

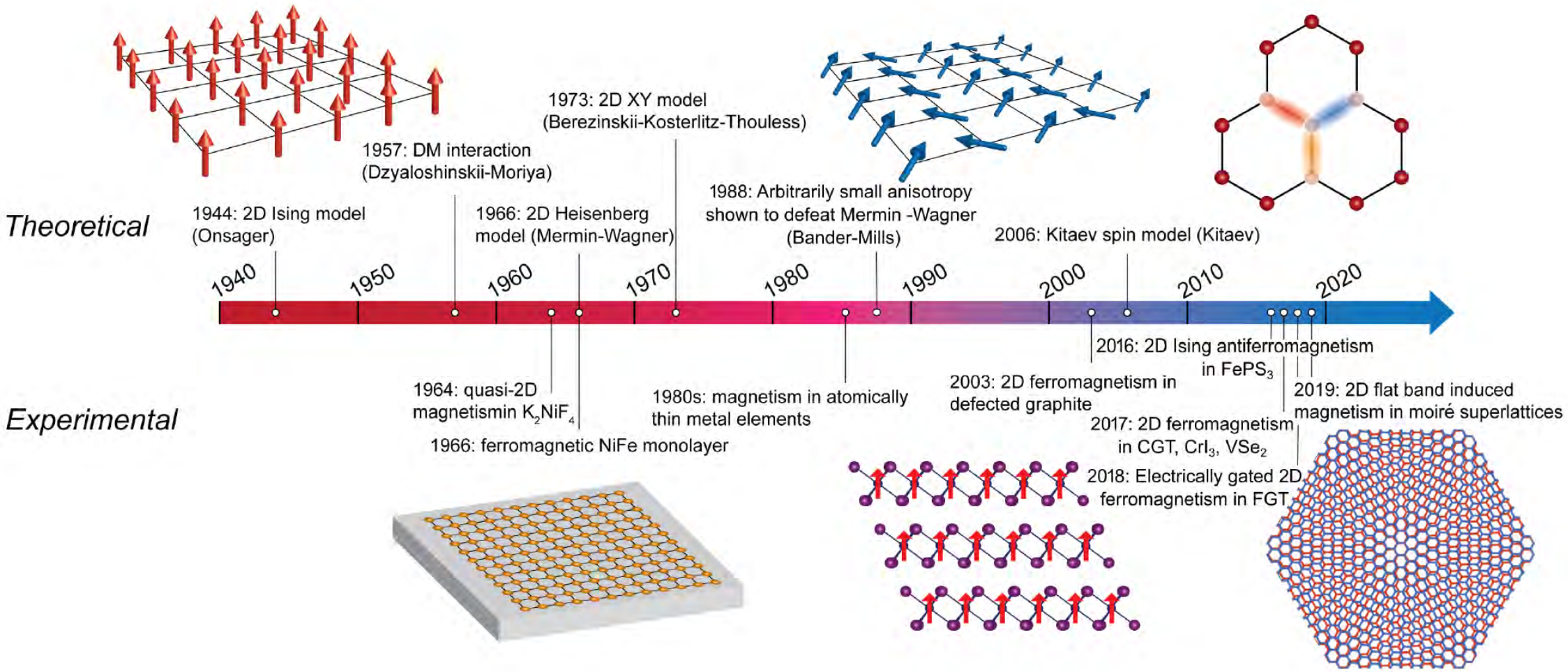

Y. Ahn et al., *Progress in Quantum Electronics* **93**, 100498 (2024).

How should we measure 2D magnets?

- Measurement techniques: neutron scattering, muon spin rotation, NMR, ESR, x-ray scattering, magnetization and susceptibility, STM, heat capacity & thermal transport

- 2D magnets contain few magnetic moments
- Correlation lengths are short

- Need techniques combining high magnetic sensitivity and spatial resolution

How to measure the magnetism of 2D systems?

Map weak magnetic field patterns with high spatial resolution

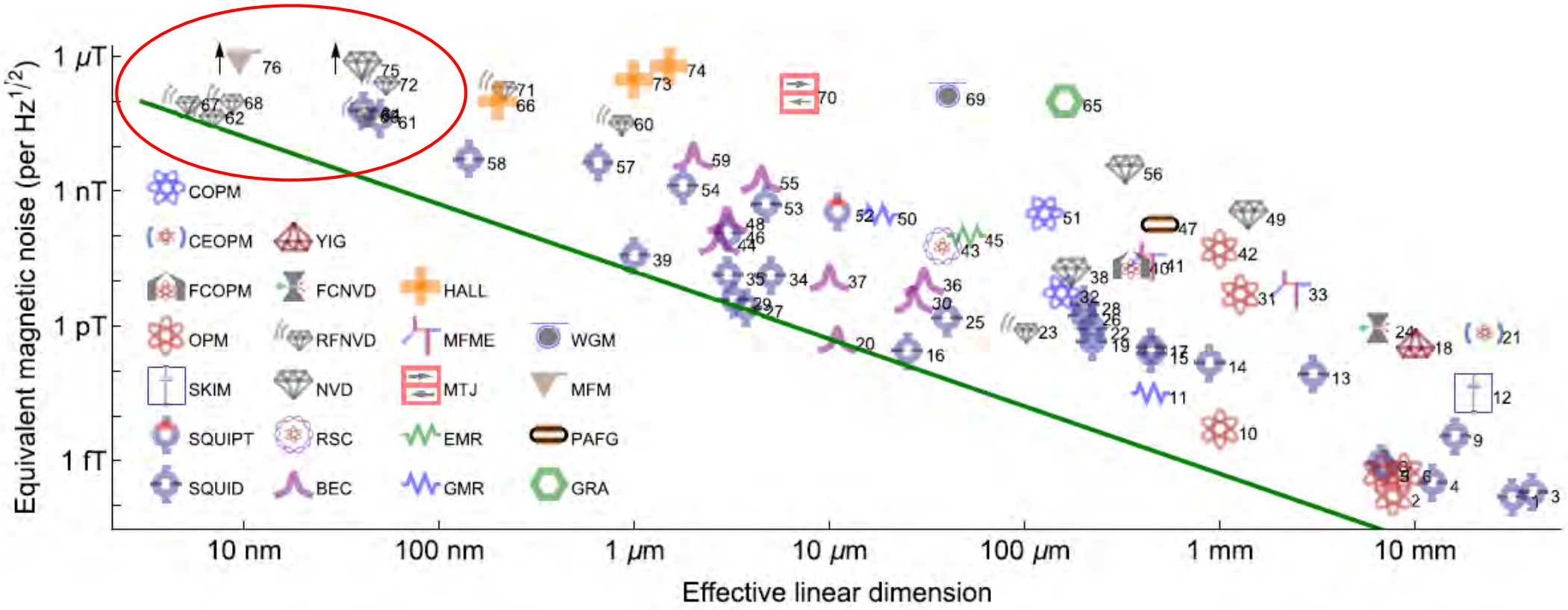

Mitchell & Palacios Alvarez, *Rev. Mod. Phys.* **92**, 021001 (2020)

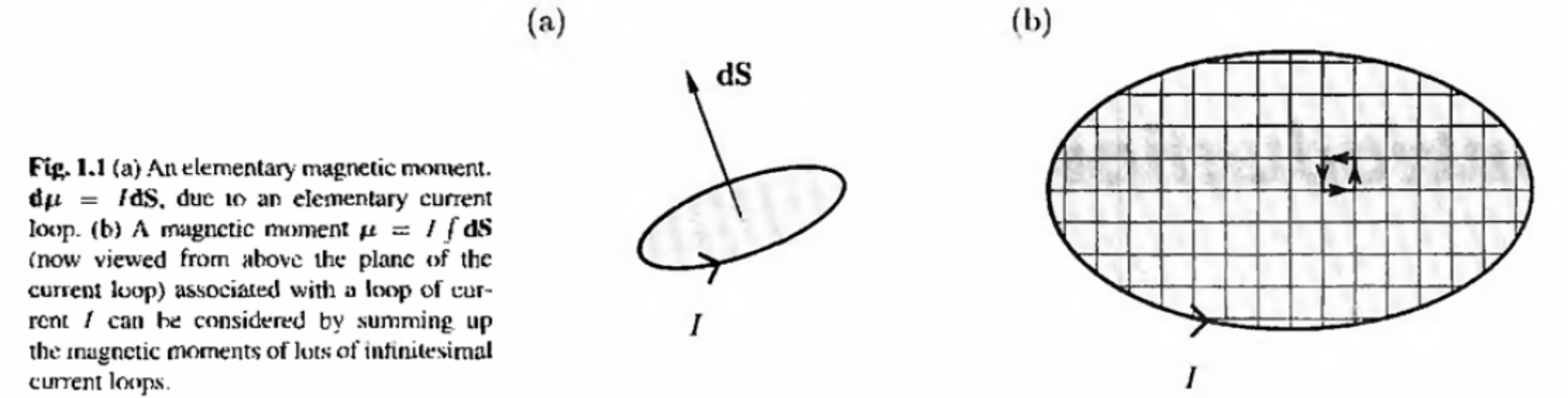

Fig. 1.1 (a) An elementary magnetic moment. $\mathbf{d}\mu = I\mathbf{dS}$, due to an elementary current loop. (b) A magnetic moment $\mu = I \int \mathbf{dS}$ (now viewed from above the plane of the current loop) associated with a loop of current I can be considered by summing up the magnetic moments of lots of infinitesimal current loops.

Magnetism in Condensed Matter, Blundell, chp. 1

Image the edges

- Out-of-plane stray field from a uniformly polarized 2D magnet

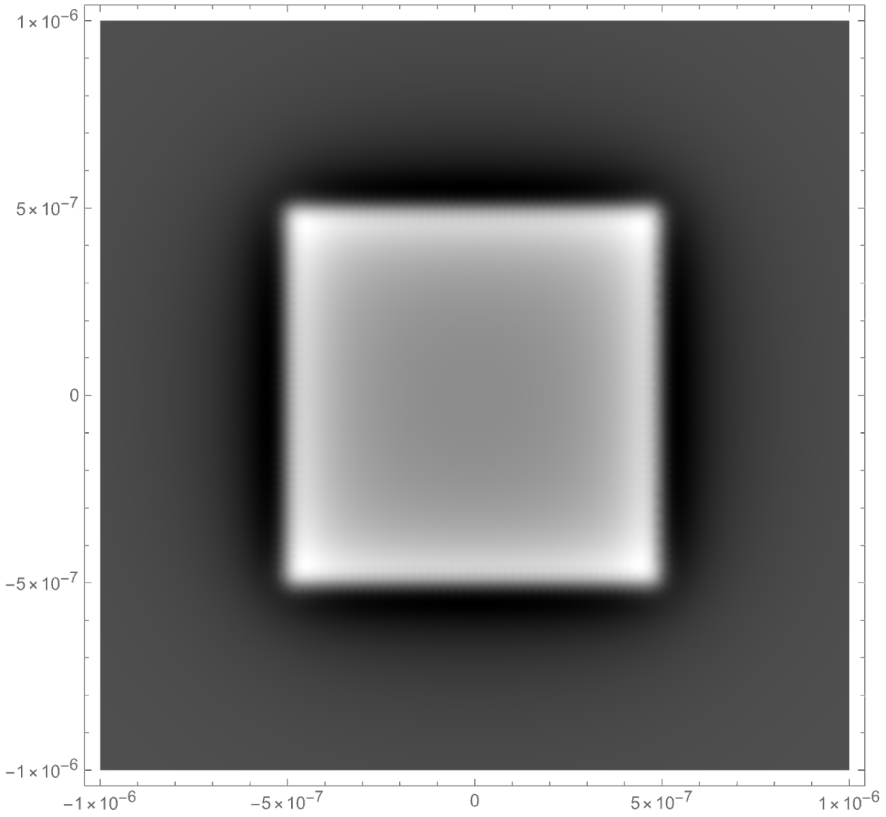

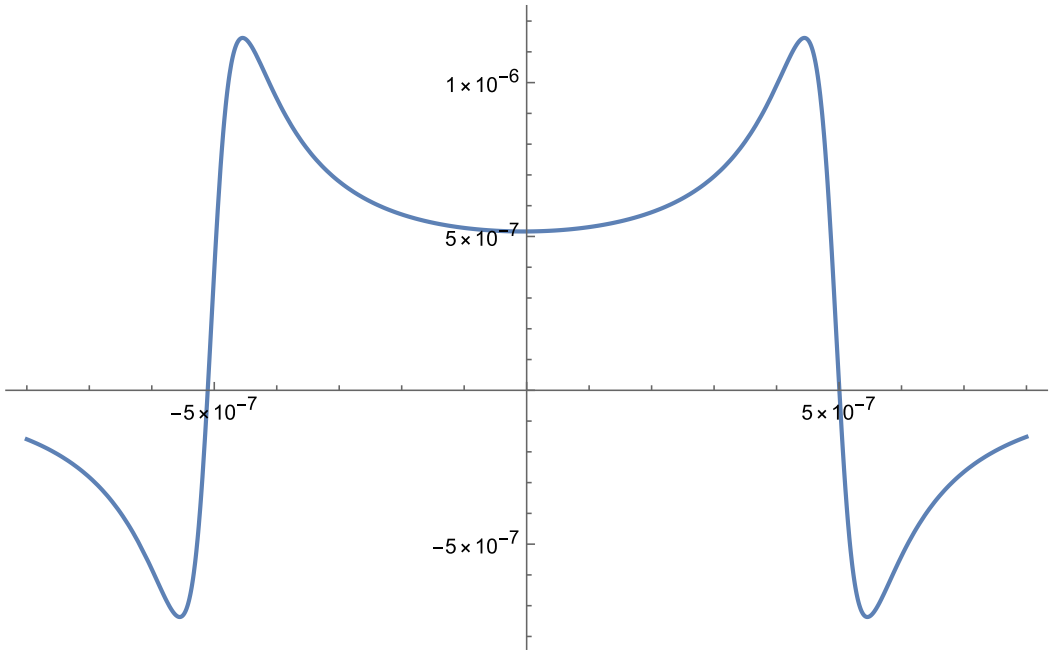

TECHNICAL
REVIEWS

Nanoscale magnetic field imaging for 2D materials

Estefani Marchiori[1], Lorenzo Ceccarelli[1], Nicola Rossi[1], Luca Lorenzelli[2], Christian L. Degen[2] and Martino Poggio[1,3]

Abstract | Nanoscale magnetic imaging can provide microscopic information about length scales, inhomogeneity and interactions of materials systems. As such, it is a powerful tool to probe phenomena such as superconductivity, Mott insulating states and magnetically ordered states in 2D materials, which are sensitive to the local environment. This Technical Review provides an analysis of weak magnetic field imaging techniques that are most promising for the study of 2D materials: magnetic force microscopy, scanning superconducting quantum interference device microscopy and scanning nitrogen-vacancy centre microscopy.

Marchiori et al., *Nat. Rev. Phys.* **4**, 49 (2022)

Magnetic imaging by "force microscopy" with 1000 Å resolution

Y. Martin and H. K. Wickramasinghe
IBM T. J. Watson Research Center, P. O. Box 218, Yorktown Heights, New York 10598

(Received 19 December 1986; accepted for publication 19 March 1987)

We describe a new method for imaging magnetic fields with 1000 Å resolution. The technique is based on using a force microscope to measure the magnetic force between a magnetized tip and the scanned surface. The method shows promise for the high-resolution mapping of both static and dynamic magnetic fields.

Appl. Phys. Lett. 50 (20), 18 May 1987

Magnetic force microscopy: General principles and application to longitudinal recording media

D. Rugar, H. J. Mamin, P. Guethner,[a] S. E. Lambert,[b] J. E. Stern,[c] I. McFadyen,[b] and T. Yogi[b]
IBM Research Division, Almaden Research Center, 650 Harry Road, San Jose, California 95120-6099

(Received 15 January 1990; accepted for publication 13 April 1990)

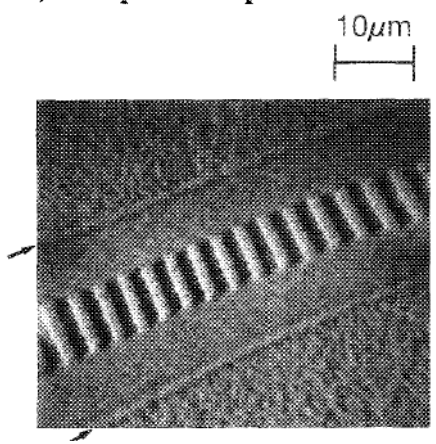

J. Appl. Phys. 68 (3), 1 August 1990

MFM achieves down to 10 nm resolution

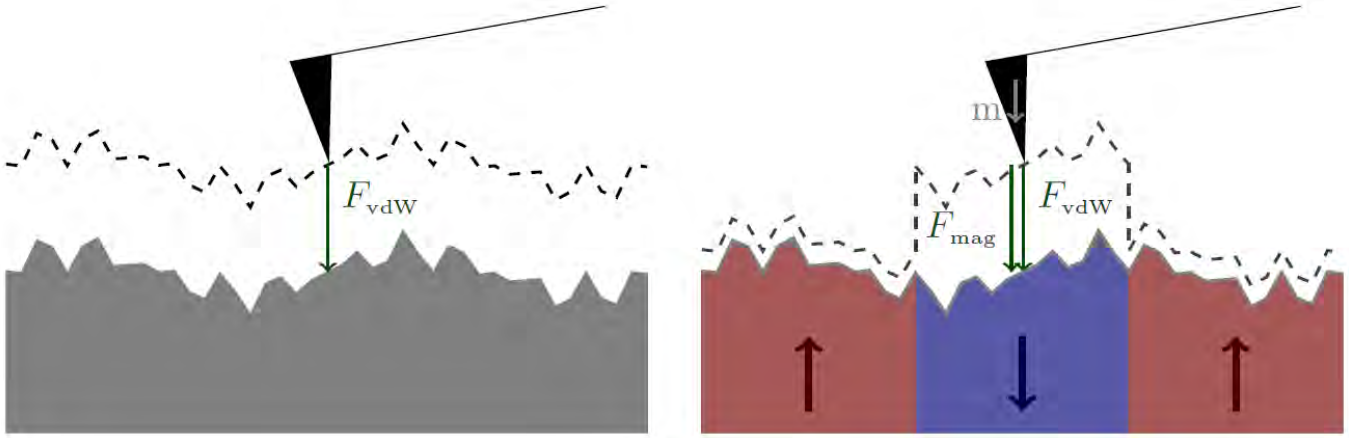

Schwenk, *Ph.D. Thesis in Physics,* University of Basel (2016).

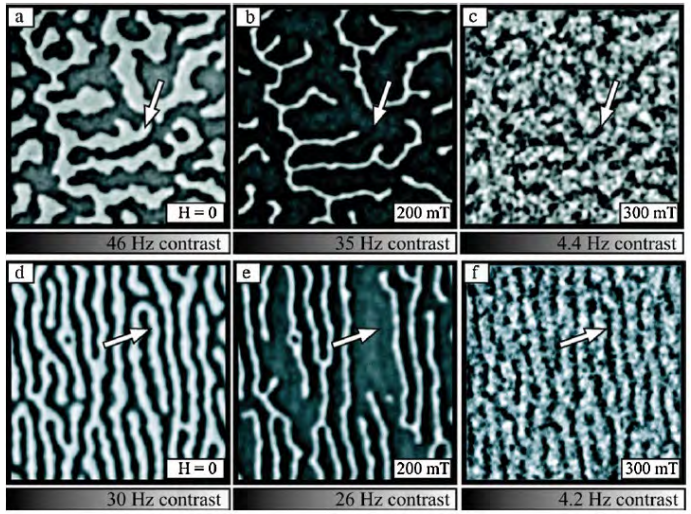

Schmid et al., *Phys. Rev. Lett.* **105**, 197201 (2010).

Nanowires as force sensors and scanning probes

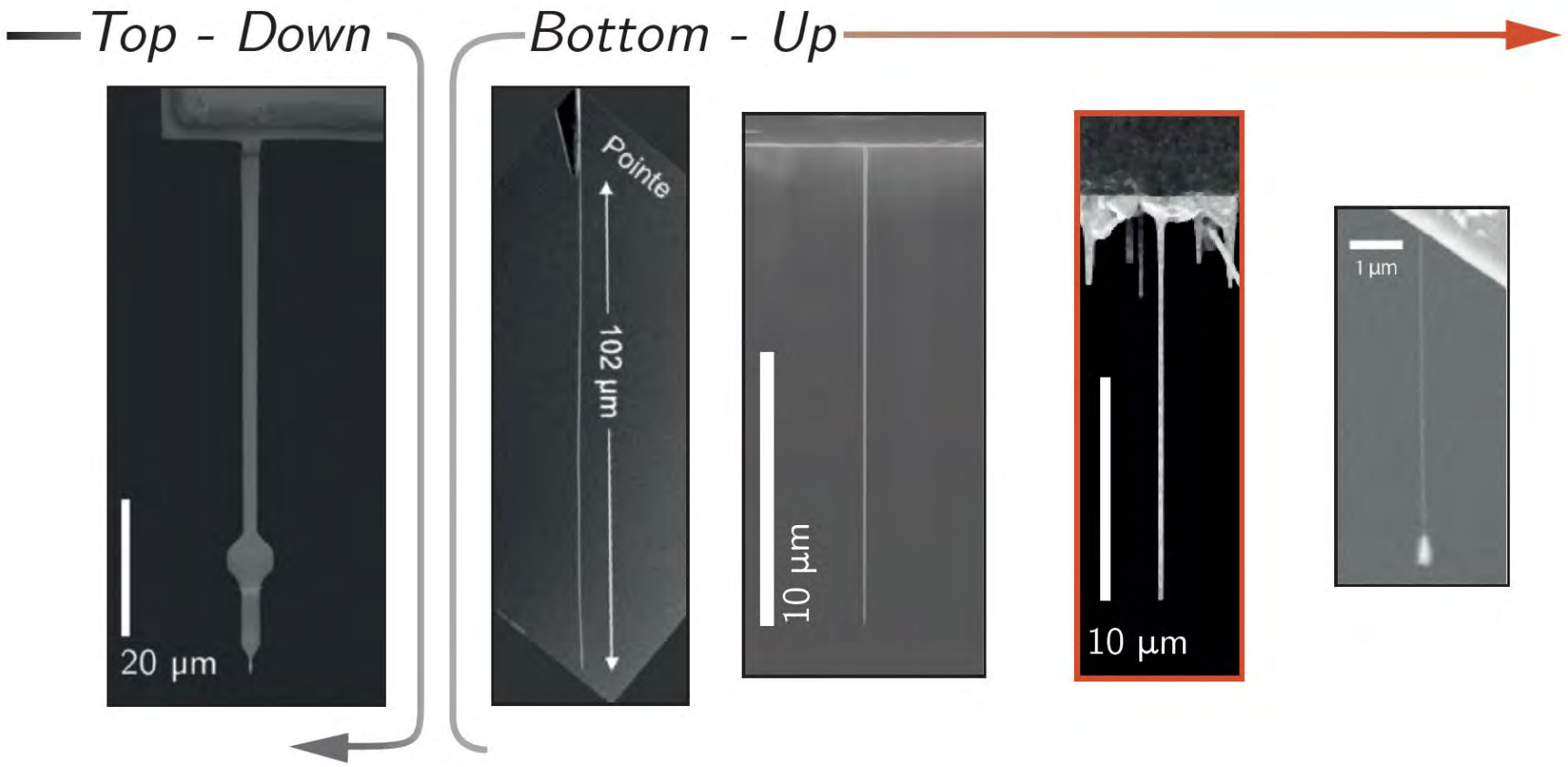

Rossi, *Ph.D. Thesis in Physics,* University of Basel (2019).

NWs with magnetic tips

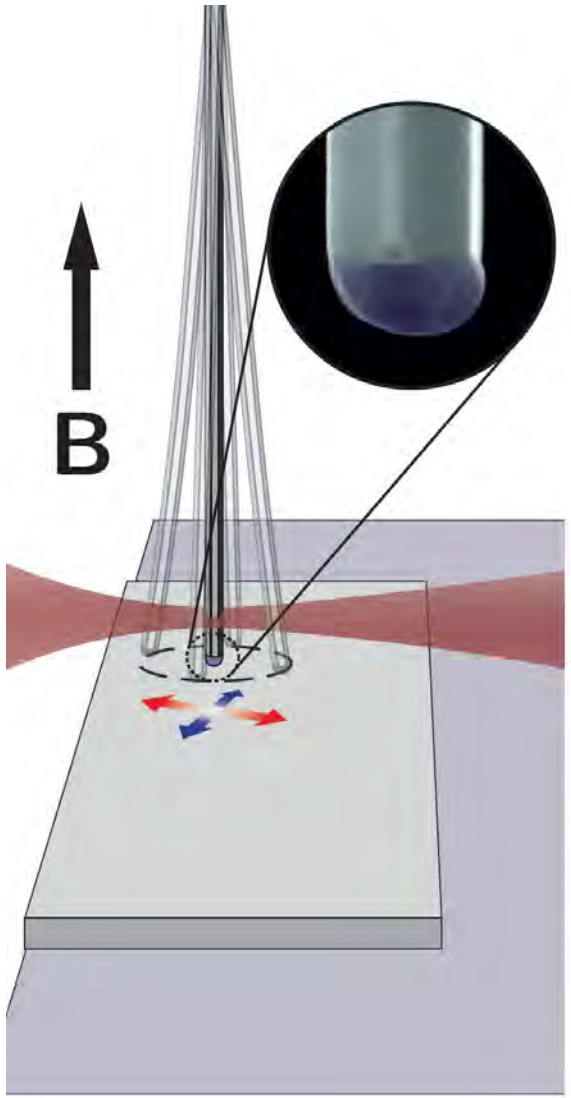

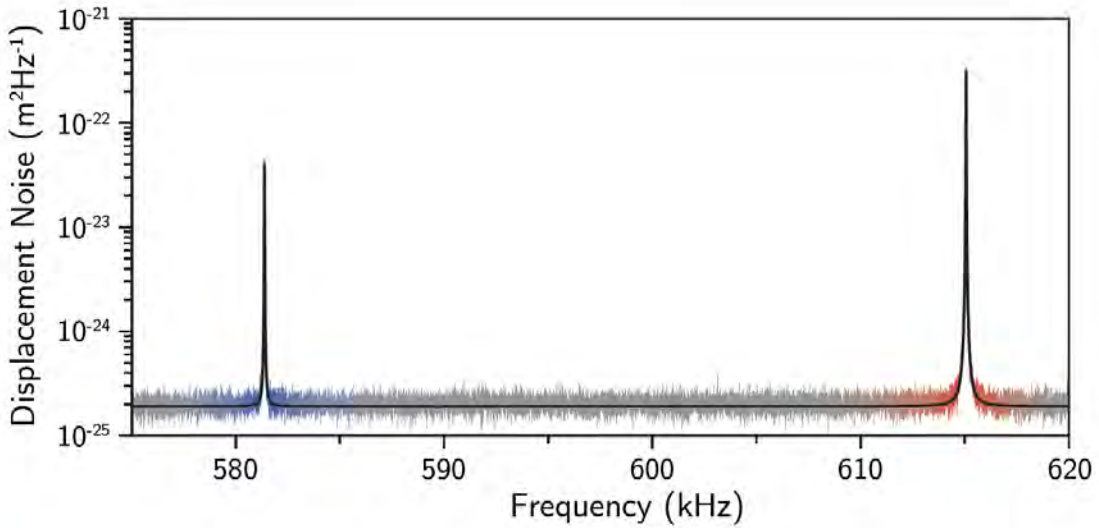

Length $\sim 17 \pm 1\,\mu$m with diameter $\sim 225 \pm 15$ nm

- $f \sim [500 - 700]$ kHz
- $Q \sim [30 - 50] \times 10^3$
- $k \sim [1 - 10]$ mN/m
- $M \sim 700$ fg
- $\Gamma \sim 50 \times 10^{-15}$ kg/s
- $F_{min} \sim 4$ aN/$\sqrt{\text{Hz}}$

Rossi et al., *Nano Lett.* **19**, 930 (2019).

Magnet-tipped nanowires as MFM probes

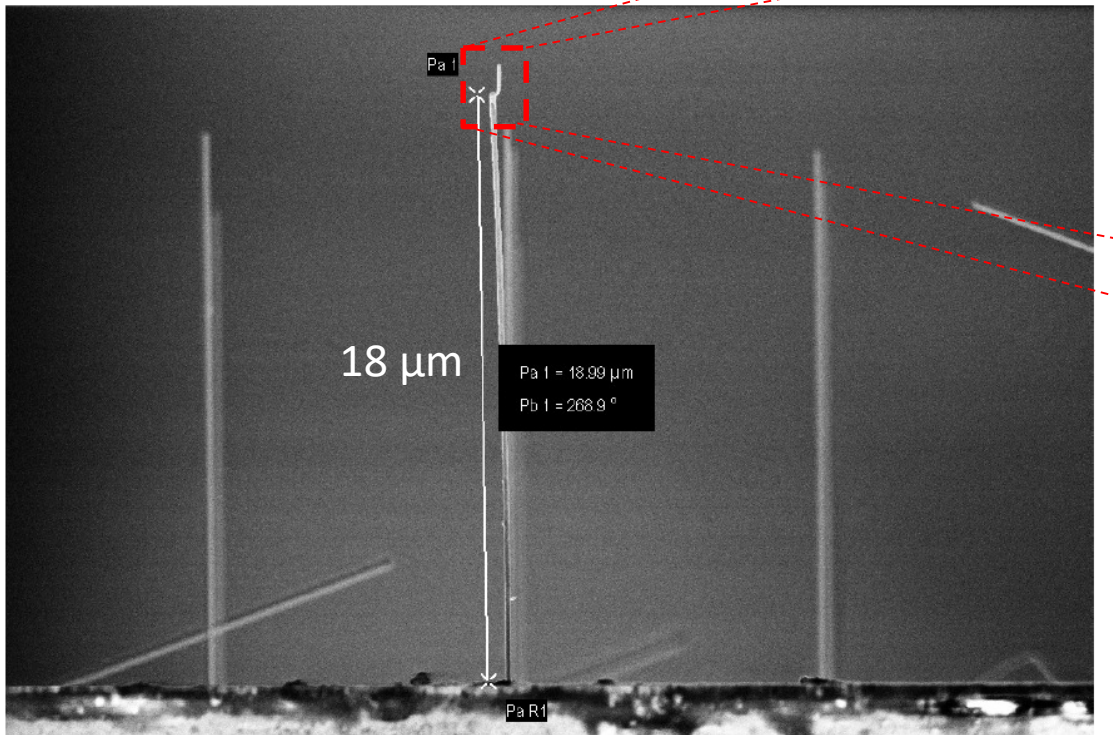

Si NWs (Budakian Group, Waterloo)

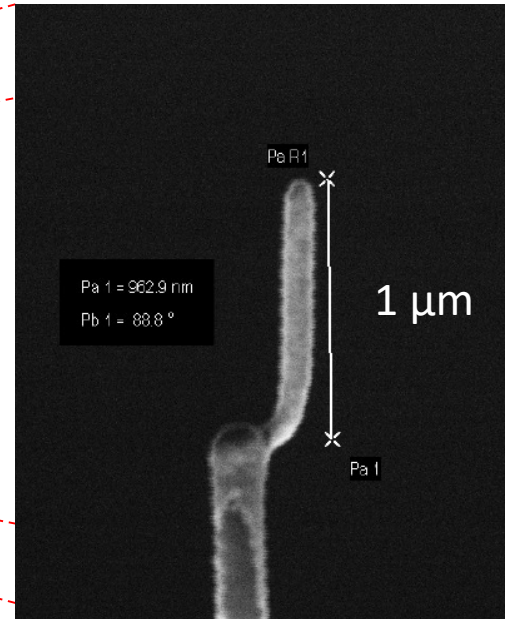

FEBID deposited Co magnetic tip

MFM

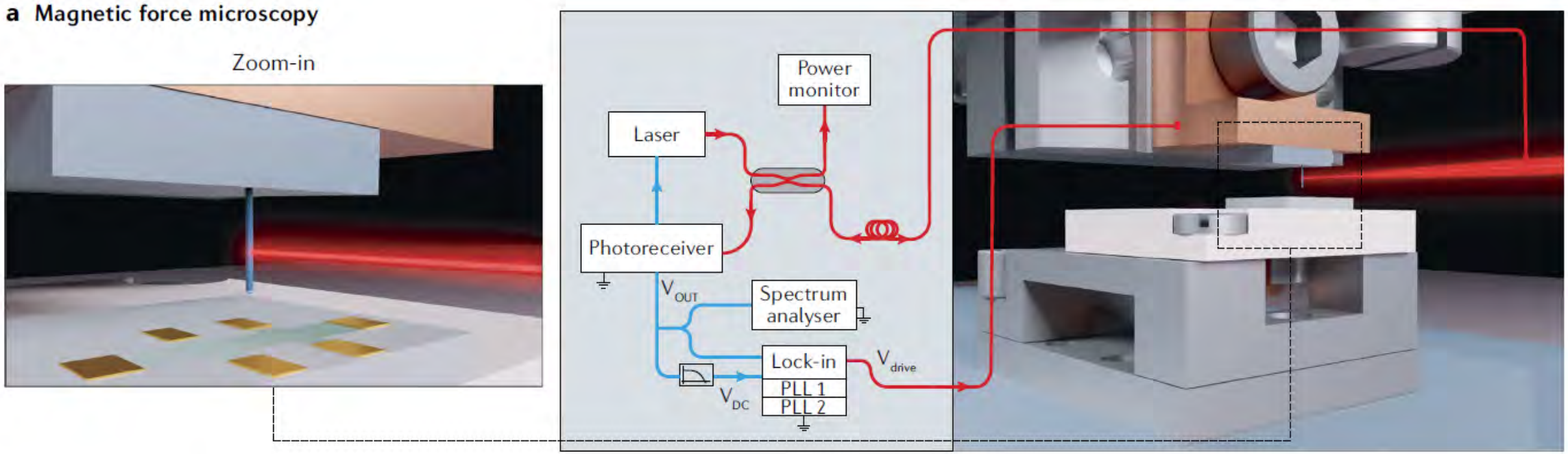
a Magnetic force microscopy
Zoom-in
Power monitor
Laser
Photoreceiver
V_{OUT}
Spectrum analyser
Lock-in
PLL 1
PLL 2
V_{drive}
V_{DC}

Magnetic Force Microscopy of bilayer $EuGe_2$

Hinrich Mattiat

Ph.D. Student

Lukas Schneider

Ph.D. Student

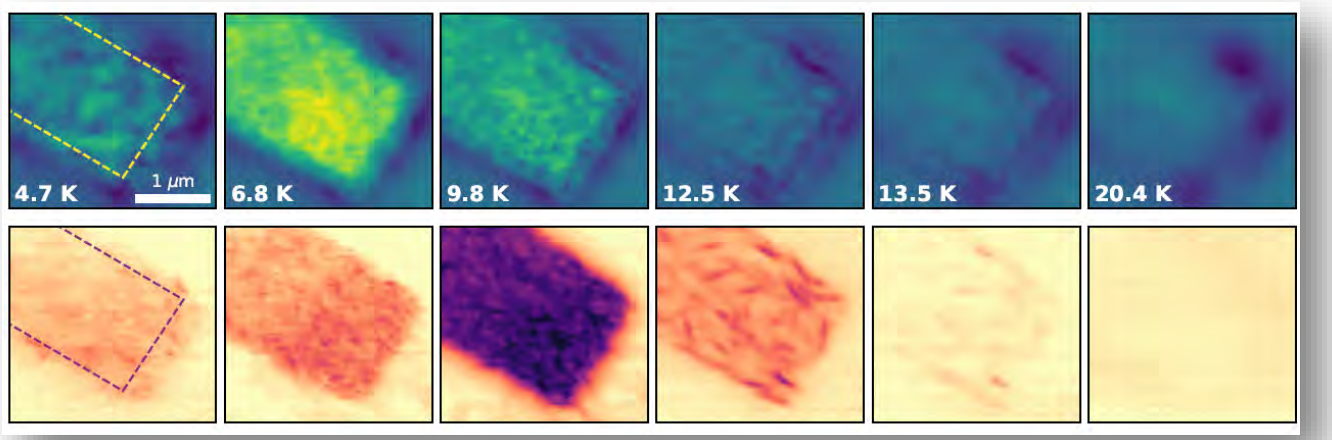

Magnetism in 2D $EuGe_2$

- Monolayer exhibits in-plane ferromagnetism (FM)
- Multi-layer (bulk) is stacked antiferromagnetically (AFM)
- layer dependent transition from AFM to FM evolves gradually from bulk to the monolayer, with evidence of a coexistence of both AFM and FM orders (exchange bias)

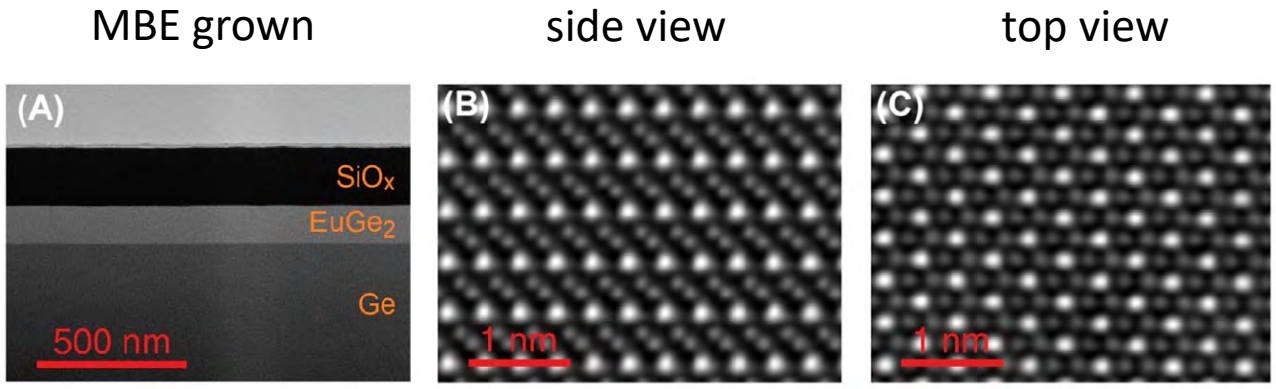

Averyanov et al., *Nano Research* **13**, 3396 (2020); Tokmachev et al., *Materials Horizons* **6**, 1488 (2019).

Bilayer $EuGe_2$: Samples

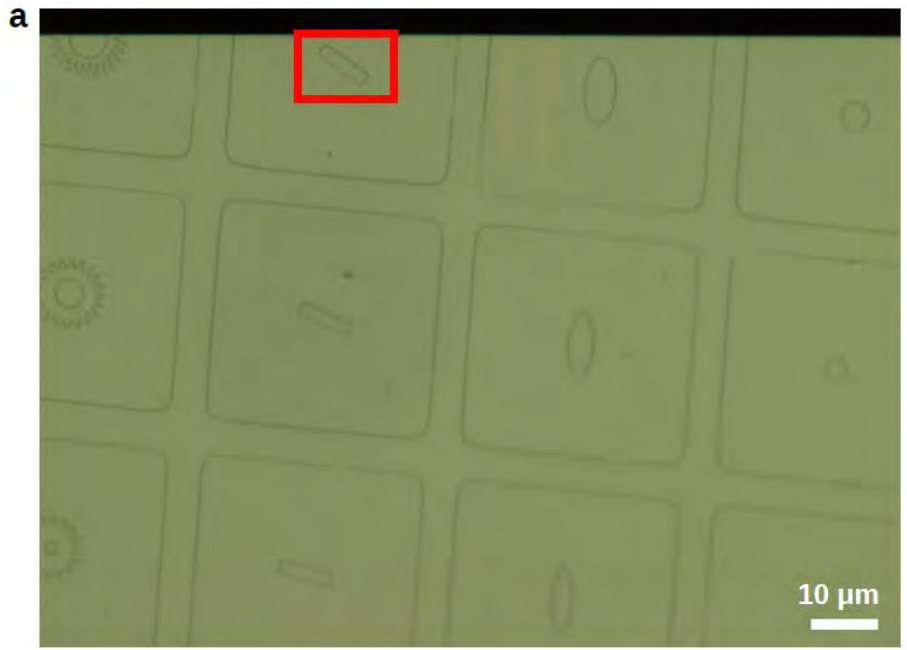

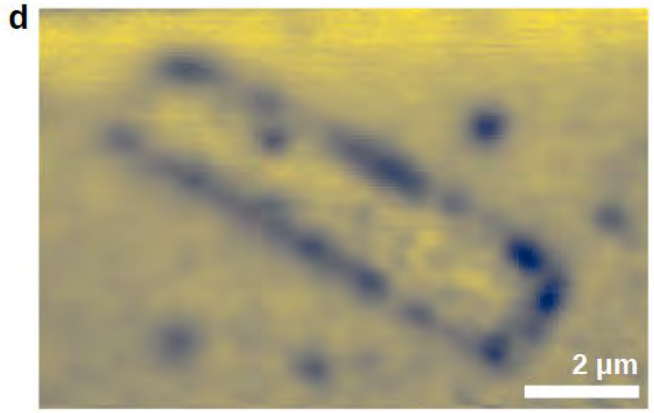

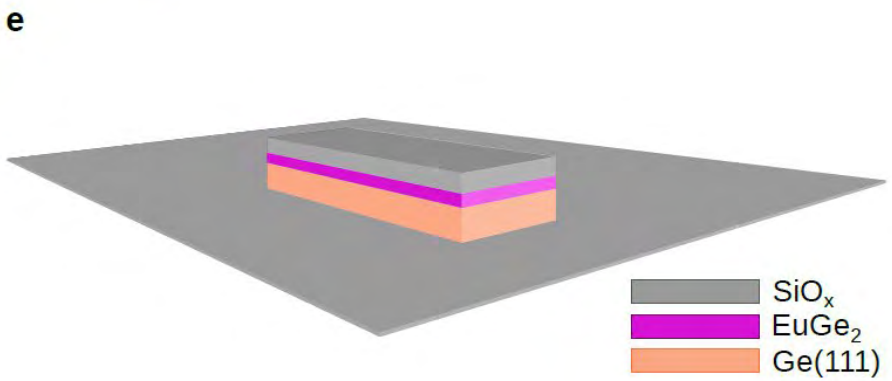

Bilayer $EuGe_2$: Applying out-of-plane field

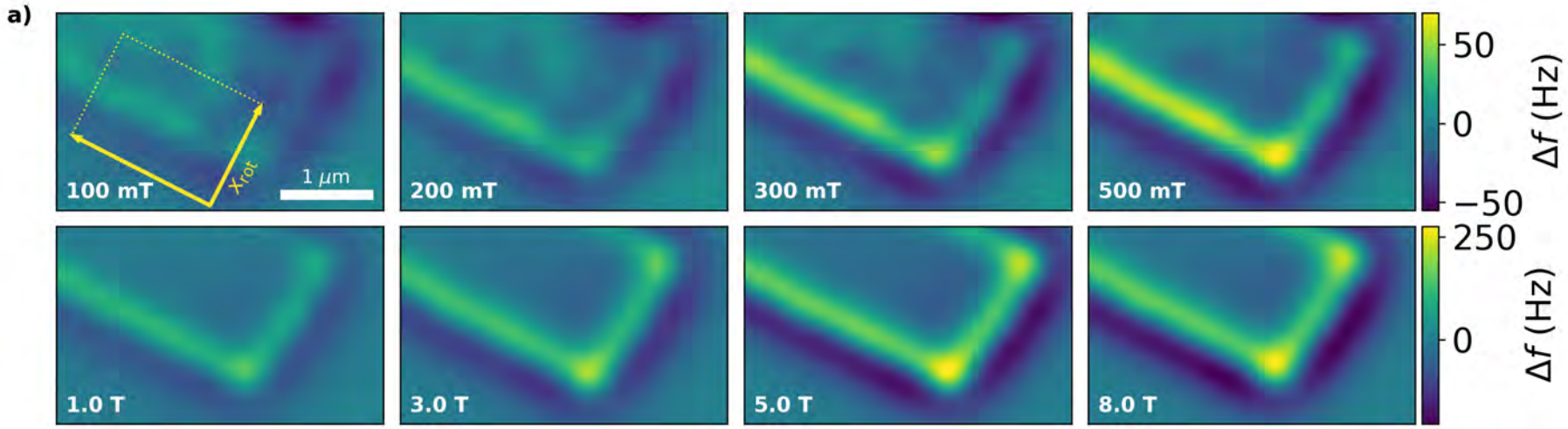

Mattiat et al., *Nanoscale* **16**, 5302 (2024).

Bilayer $EuGe_2$: Temperature dependence

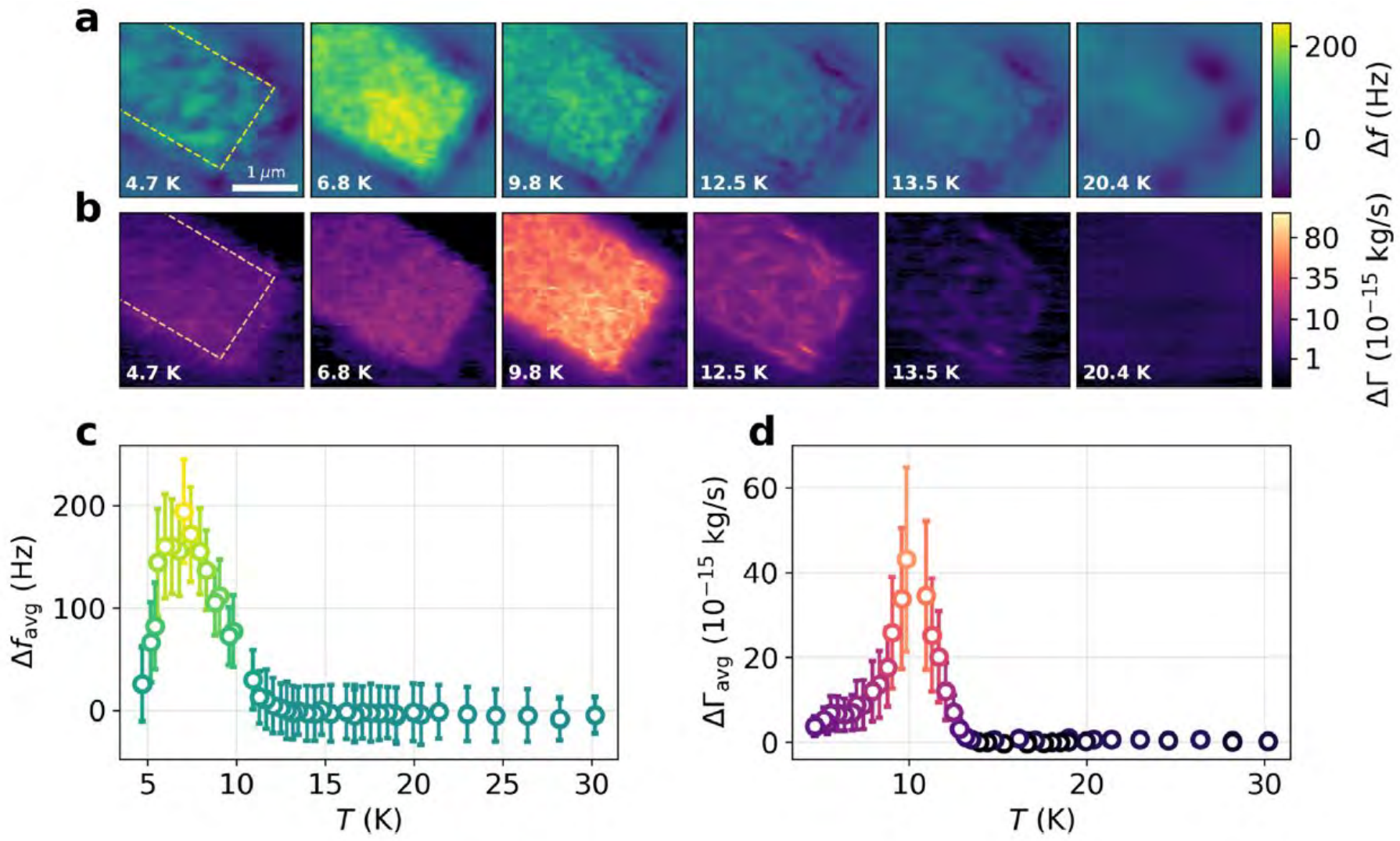

Mattiat et al., *Nanoscale* **16**, 5302 (2024).

Superconducting quantum interference device (SQUID)

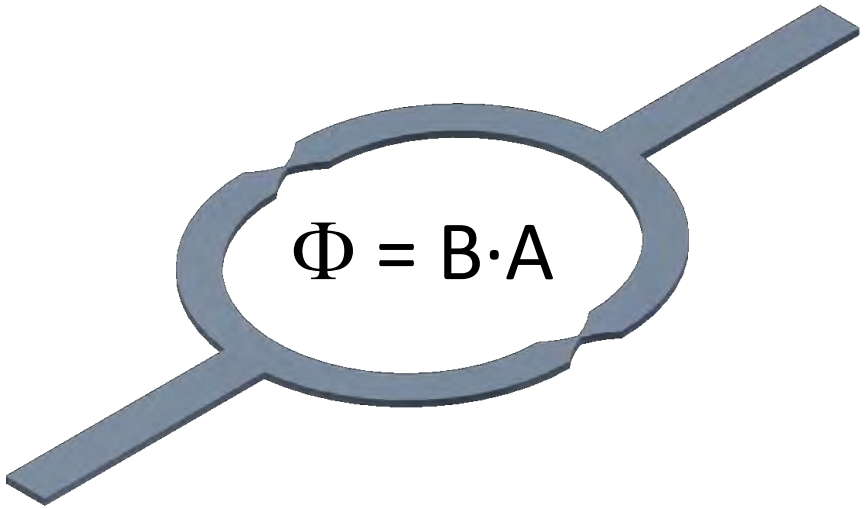

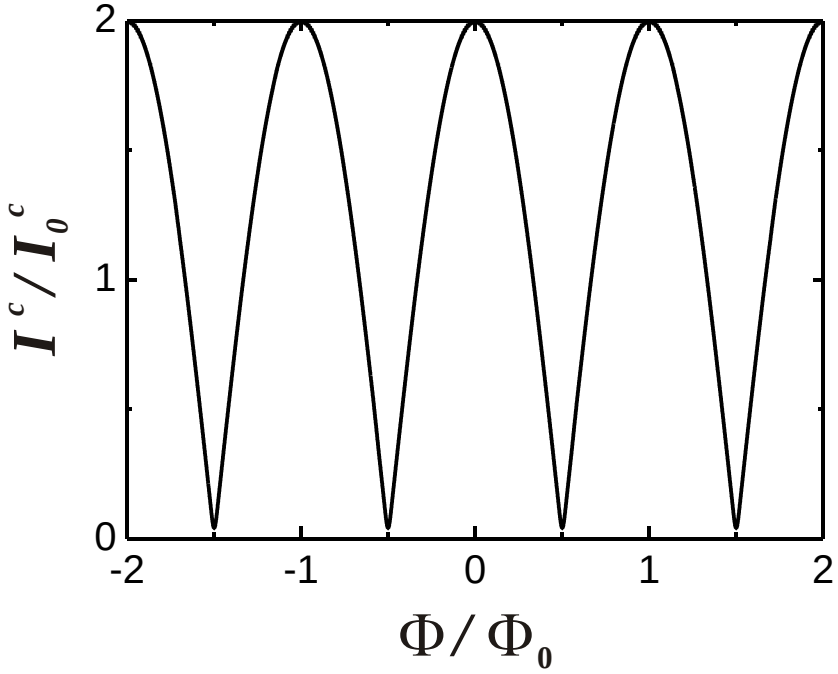

SQUID critical current: $I^c(\Phi) = 2I_0^C \cos|\square \quad / \Phi_0|$

SCANNING SQUID MICROSCOPY

John R. Kirtley
IBM T. J. Watson Research Center, Yorktown Heights, New York 10598;
e-mail: kirtley@watson.ibm.com

John P. Wikswo, Jr.
Department of Physics and Astronomy, Vanderbilt University, Nashville,
Tennessee 37235; e-mail: wikswojp@ctrvax.vanderbilt.edu

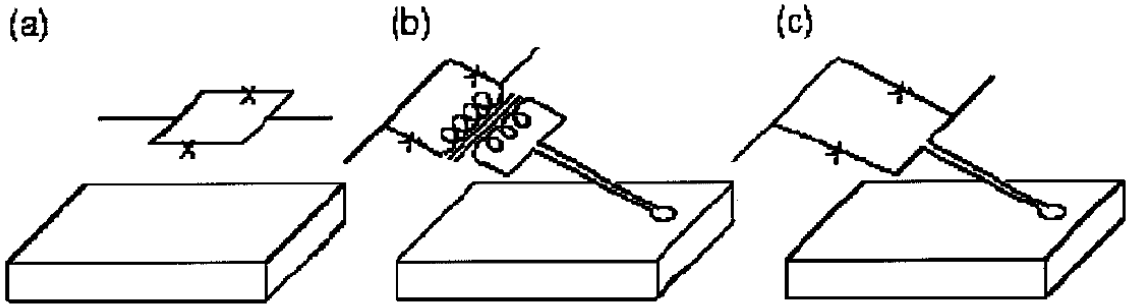

Annu. Rev. Mater. Sci. 1999. 29:117–48

2024 roadmap on magnetic microscopy techniques and their applications in materials science

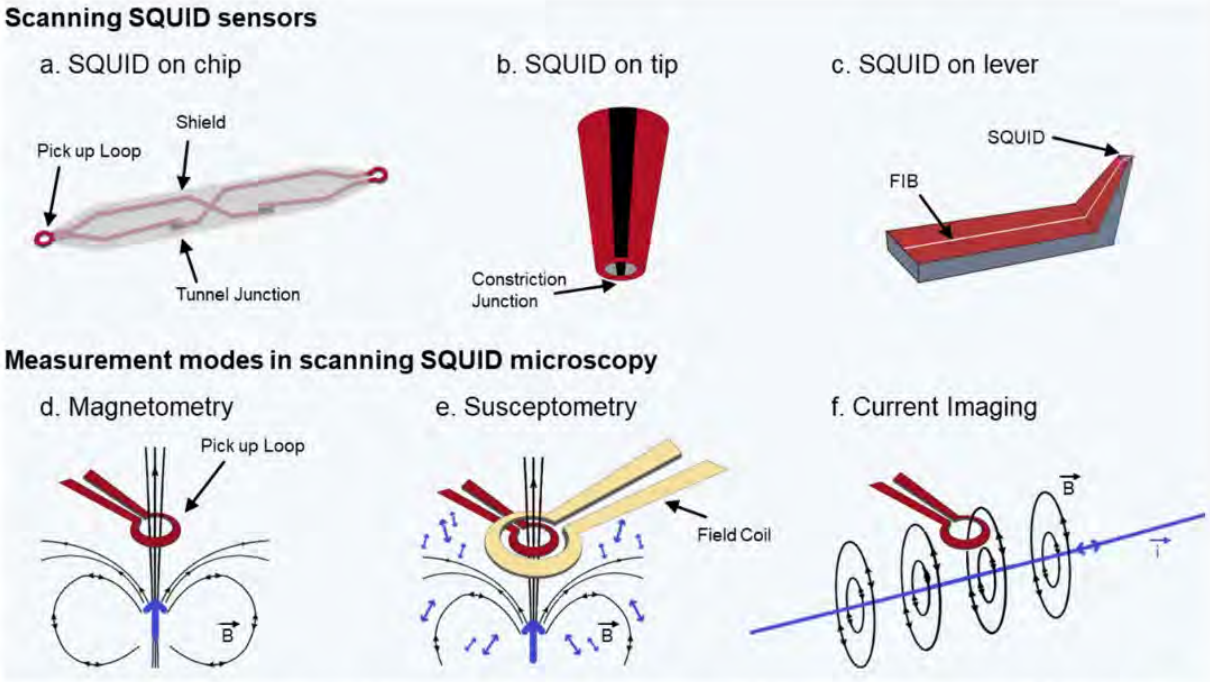

Figure 1. Scanning SQUID sensors and operation modes. (a)–(c) Illustration of three sensor realisations: (a) SQUID on chip (SOC) (b) SQUID on tip (SOT) (c) SQUID on lever (SOL). (d)–(f) Measurement modes in SSM. In (d) magnetometry, the SQUID's pick-up loop captures the magnetic field lines penetrating its area. By rastering the pick-up loop above the sample's surface we generate a map of the local magnetic flux. In (e) susceptometry, current flowing through a single turn field coil concentric with the pick-up loop creates a magnetic field at the sample's surface. The sample's response to this field is sensed by the pick-up loop. By modulating the field coil current we lock into the response, allowing for simultaneous measurement of magnetometry and susceptometry. In (f) current imaging, the magnetic fields generated by the current flow are imaged, allowing for reconstruction of the current density map.

Christensen et al., *J. Phys. Mater.* **7**, 032501 (2024)

Self-Aligned Nanoscale SQUID on a Tip

Amit Finkler,*,† Yehonathan Segev,† Yuri Myasoedov,† Michael L. Rappaport,† Lior Ne'eman,† Denis Vasyukov,† Eli Zeldov,† Martin E. Huber,‡ Jens Martin,§ and Amir Yacoby§

†Department of Condensed Matter Physics, Weizmann Institute of Science, Rehovot 76100, Israel, ‡Departments of Physics and Electrical Engineering, University of Colorado, Denver, Colorado 80217, and §Department of Physics, Harvard University, Cambridge, Massachusetts 02138

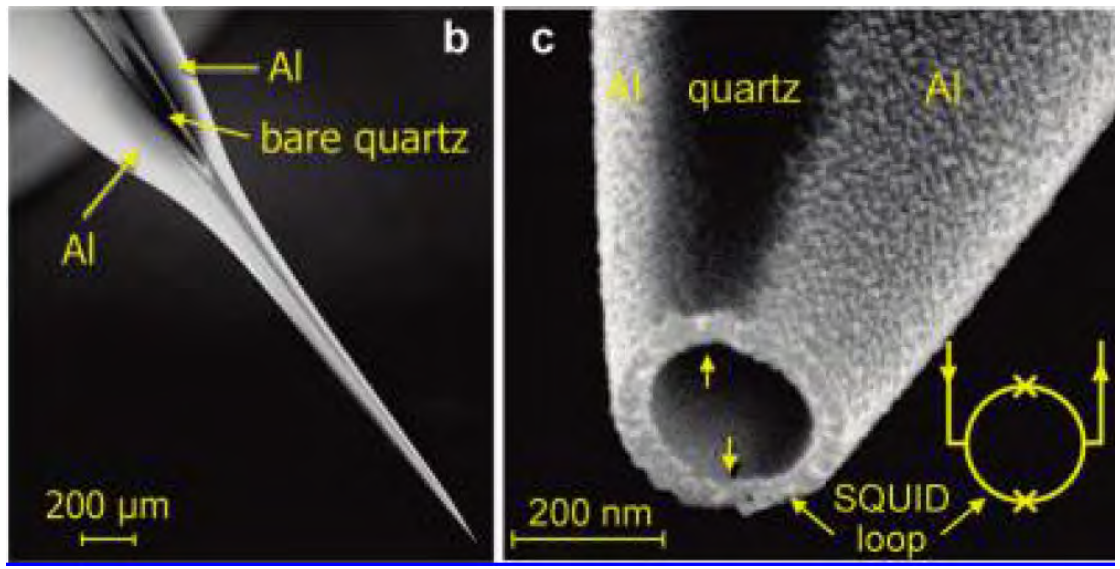

Nano Lett. **2010,** *10,* 1046–1049

SQUID-on-tip sensor

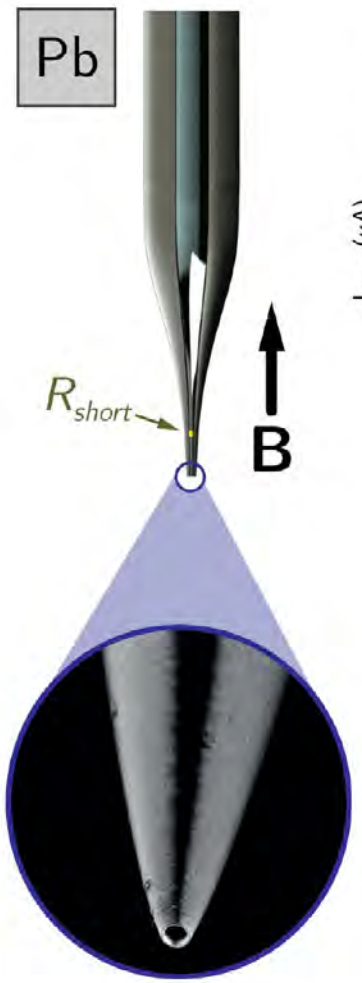

spatial res: 50-200 nm

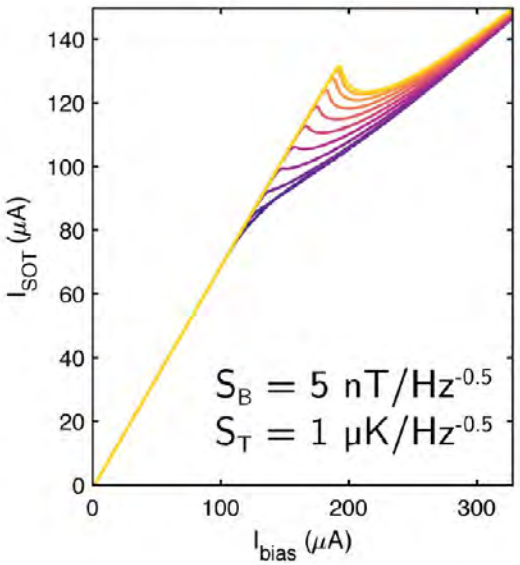

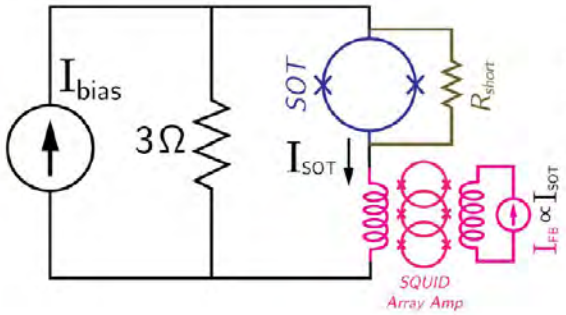

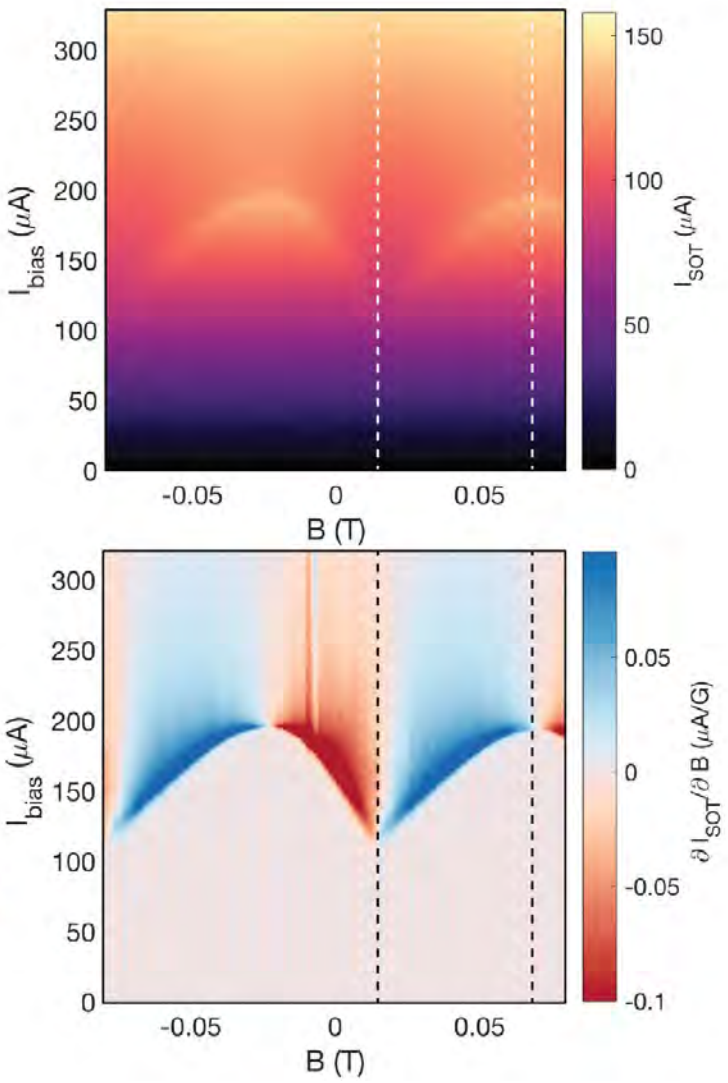

Vasyukov et al., *Nat. Nanotechnol.* **8**, 639 (2013)

SQUID-on-Cantilever

Limitation: SQUID-on-tip with Tuning fork

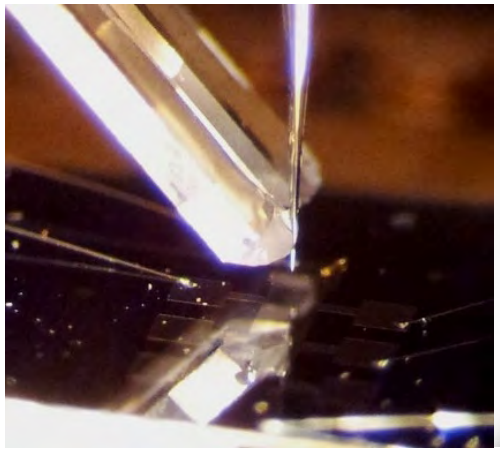

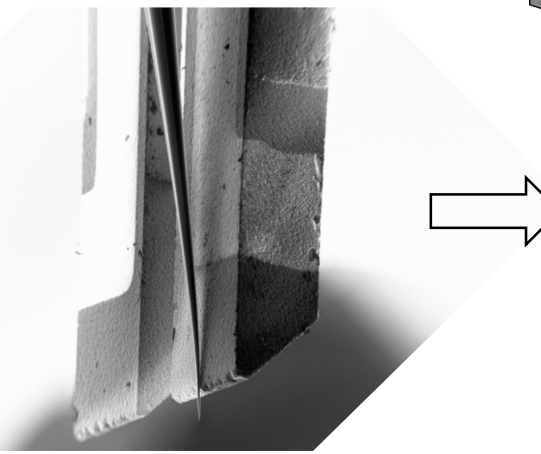

SQUID + Atomic Force Microscopy

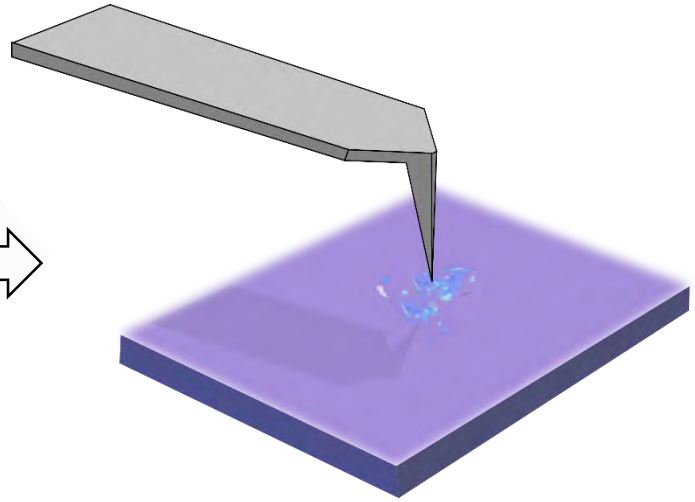

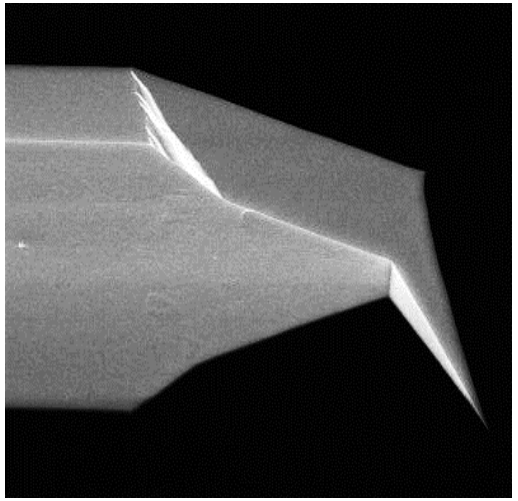

Sensitive to the surface **~ 10-20 nm**

Tip sample distance control **~ 1 µm**

Frequency shift

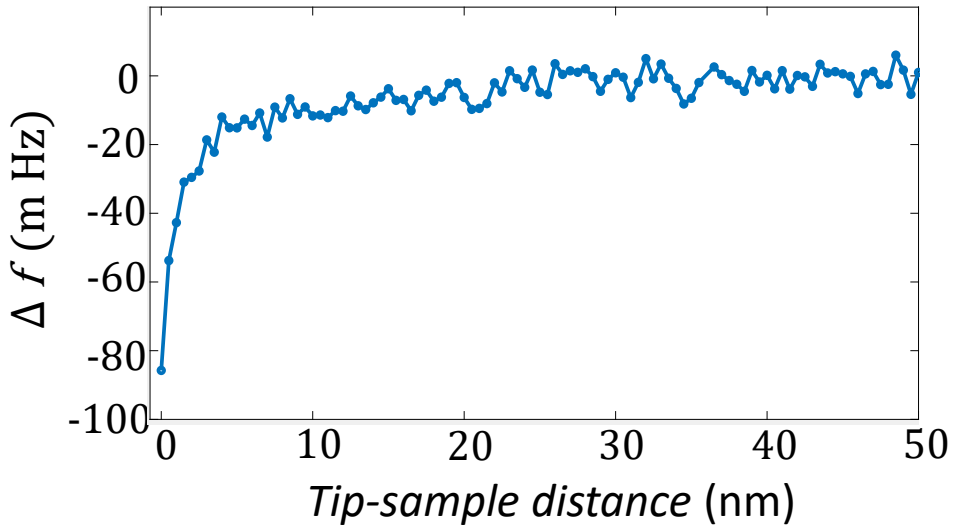

Frequency shift

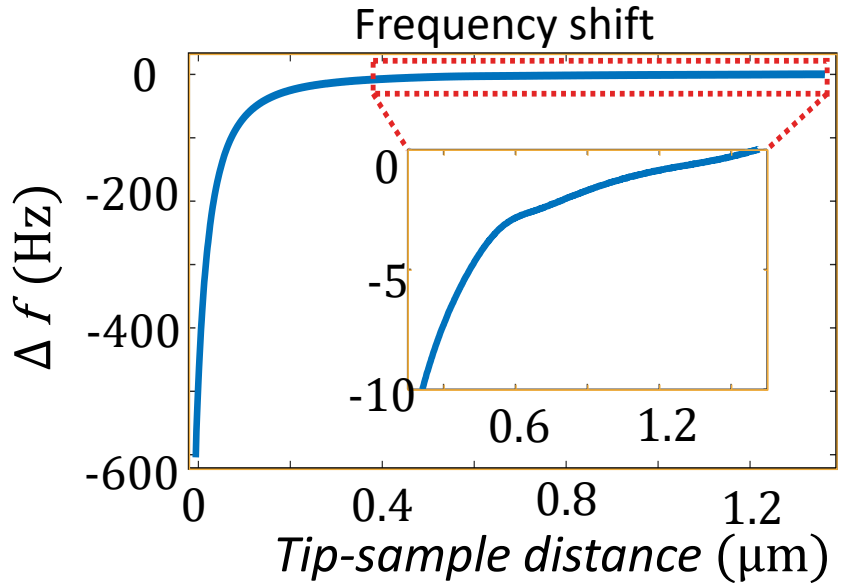

Fabrication of SQUID-on-lever

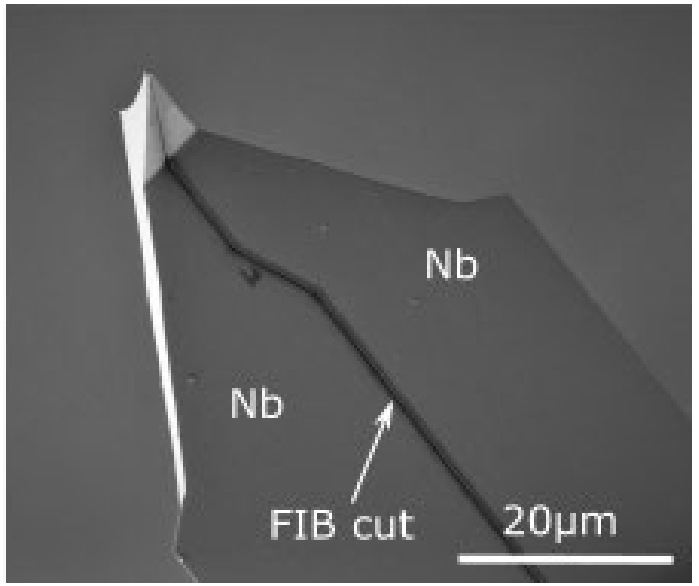

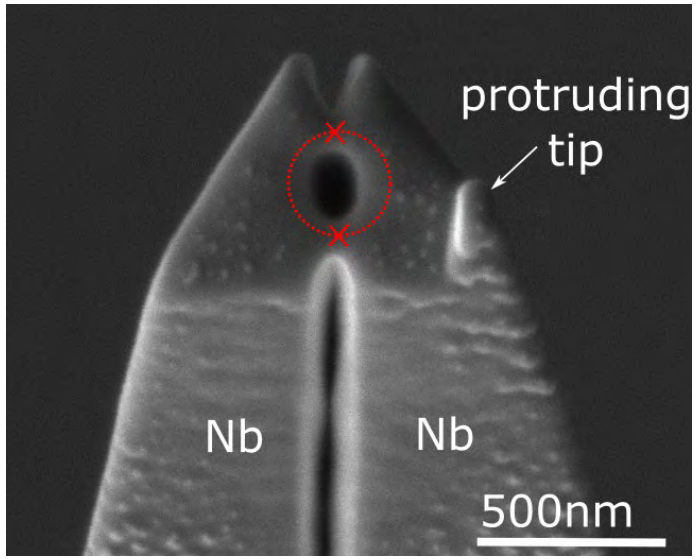

Effective diameter ~ 150 - 350 nm

M. Wyss et al. Phys. Rev. Appl. 17, 034002 (2022)

Magnetic and Thermal Sensitivity

I-V Characteristics (T = 4.2 K)

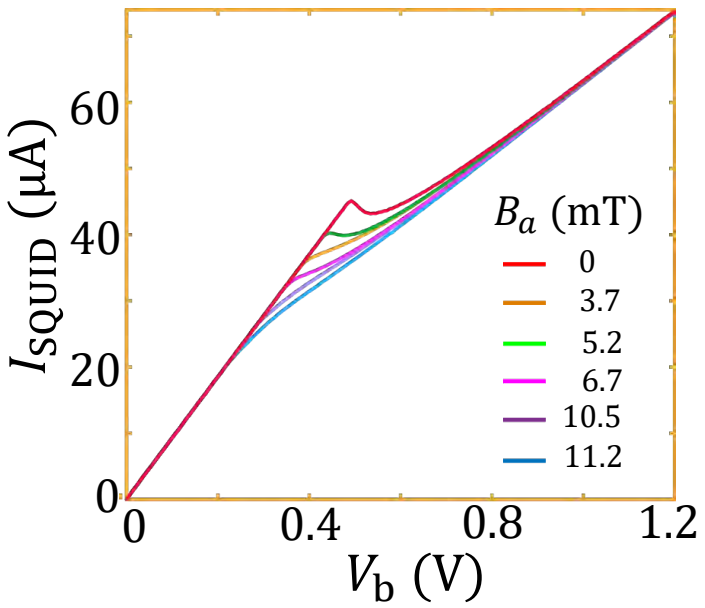

Quantum Interference

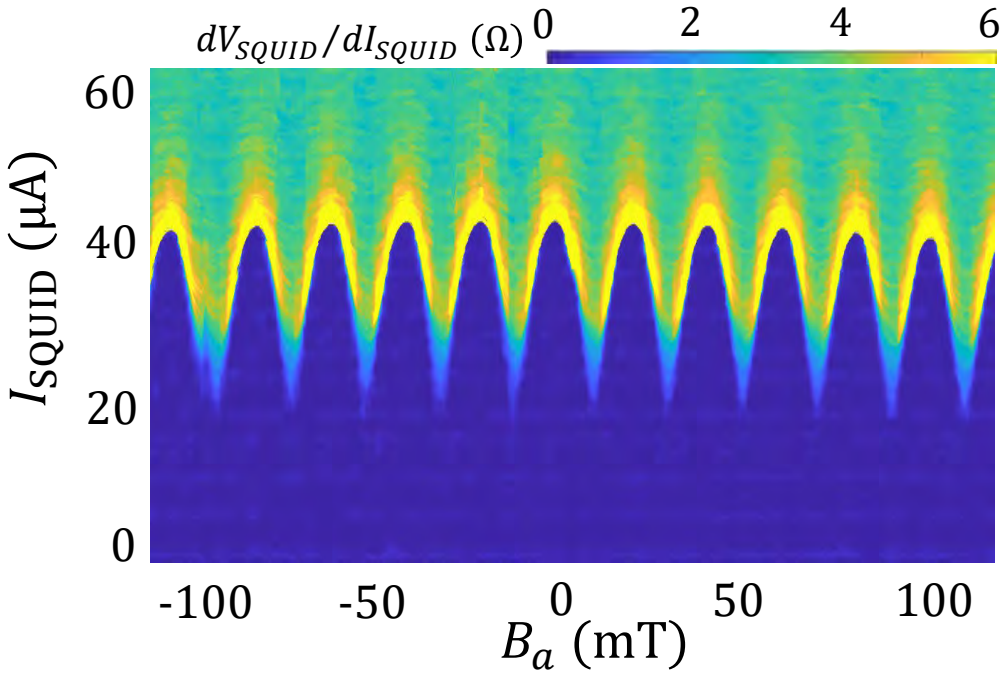

Flux Sensitivity, $S_{\Phi}^{1/2} \sim 0.2\,\mu\Phi_0/\mathrm{Hz}^{1/2}$

Temperature Sensitivity, $S_{\mathrm{T}}^{1/2} \sim 600\,\mathrm{nK}/\mathrm{Hz}^{1/2}$

M. Wyss et al. Phys. Rev. Appl. 17, 034002 (2022)

Scanning SQUID on Cantilever Microscopy

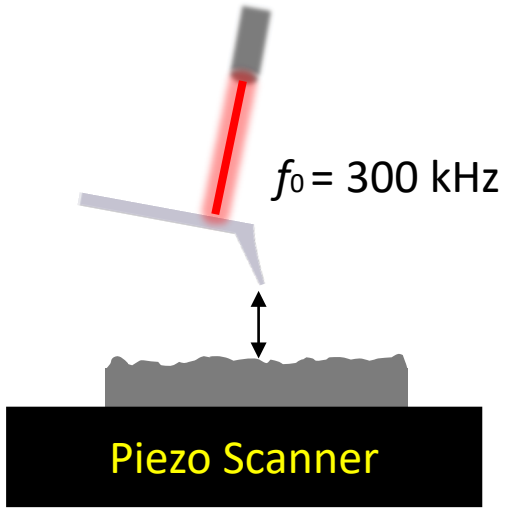

Home-built scanning probe microscope

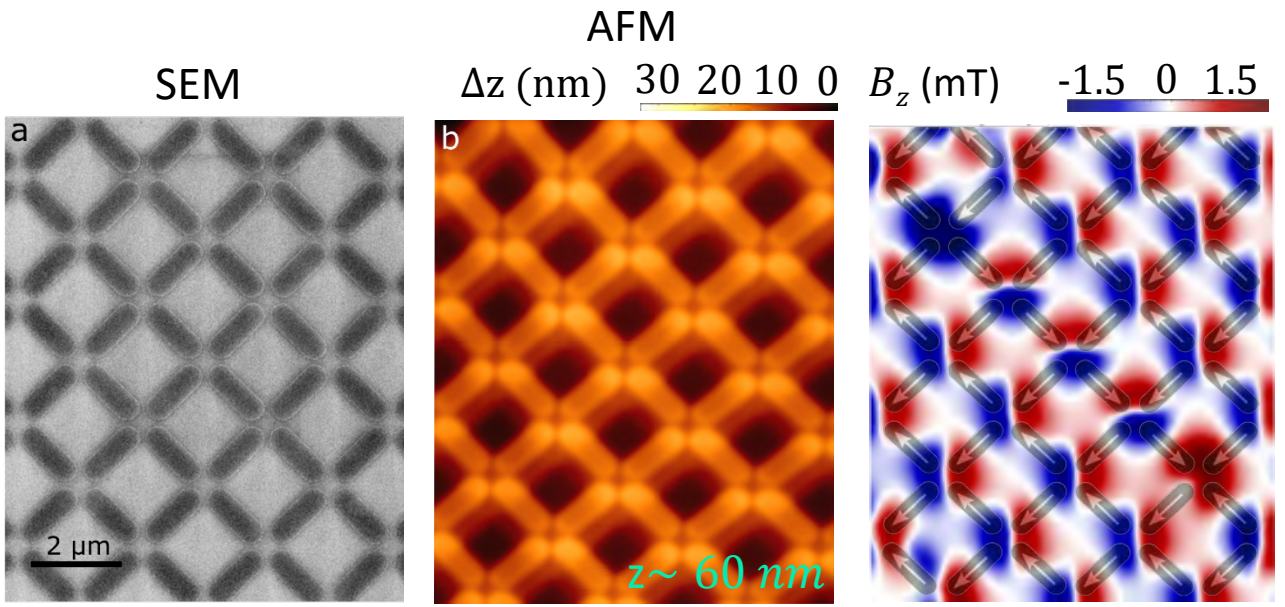

M. Wyss et al. Phys. Rev. Appl. 17, 034002 (2022)

Reducing the size of SQUID on lever

d = 30
$d_{eff} \approx$

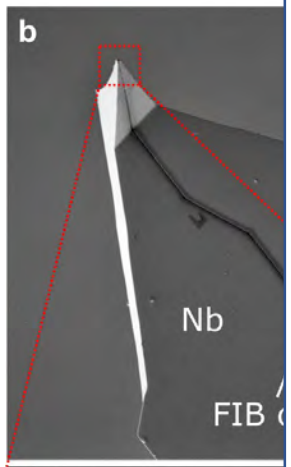

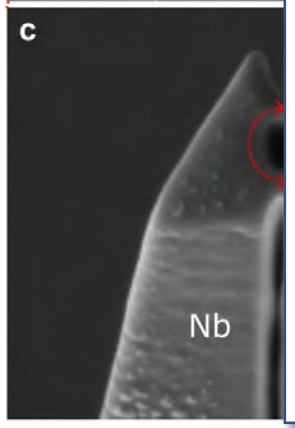

José María
De Teresa (Zaragoza)

Dieter Kölle
(Tübingen)

Armin Knoll
(IBM Zürich)

Universität Basel

CSIC

EBERHARD KARLS
UNIVERSITÄT
TÜBINGEN

IBM

FIBsuperProbes

Funded by
the European Union

fibsuperprobes.com

Sub 100-nm spatial resolution

Cu_2OSeO_3

- Helical, conical and skyrmion phases
- Lengthscale of helimagnetic order: 62 nm

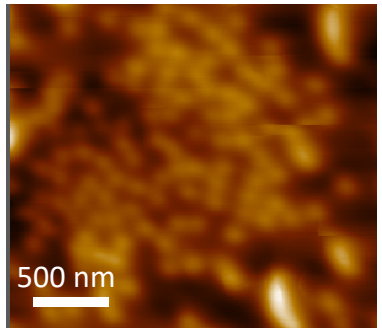

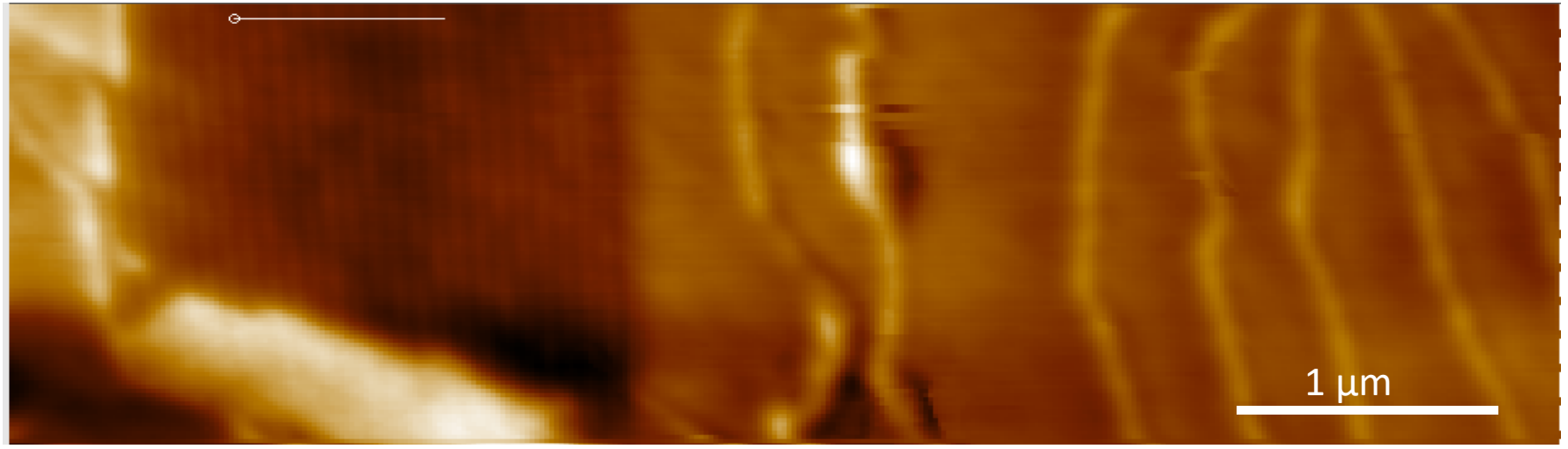

In preparation.

Scanning SQUID microscopy of strained 2D CrSBr

Dr. Kousik Bagani

Post-doctoral Researcher

Andriani Vervelaki

Ph.D. Student

Daniel Jetter

Ph.D. Student

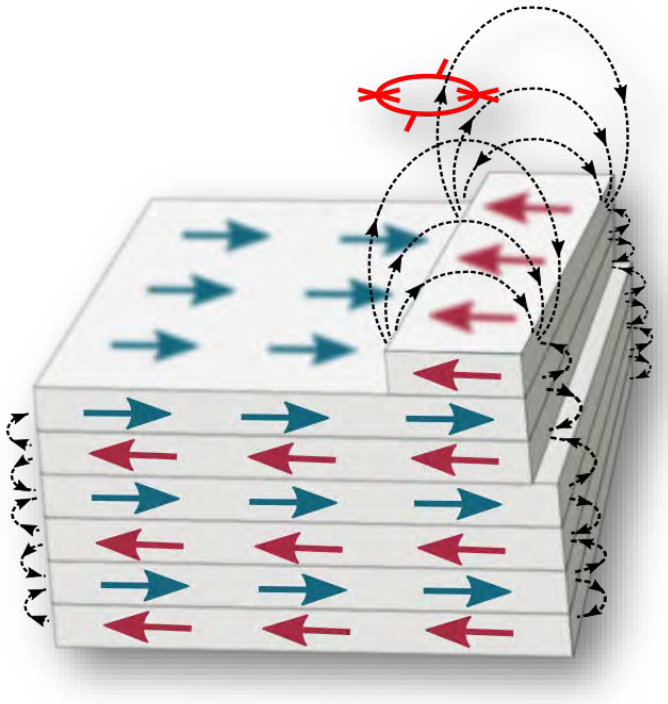

Strain response of 2D CrSBr

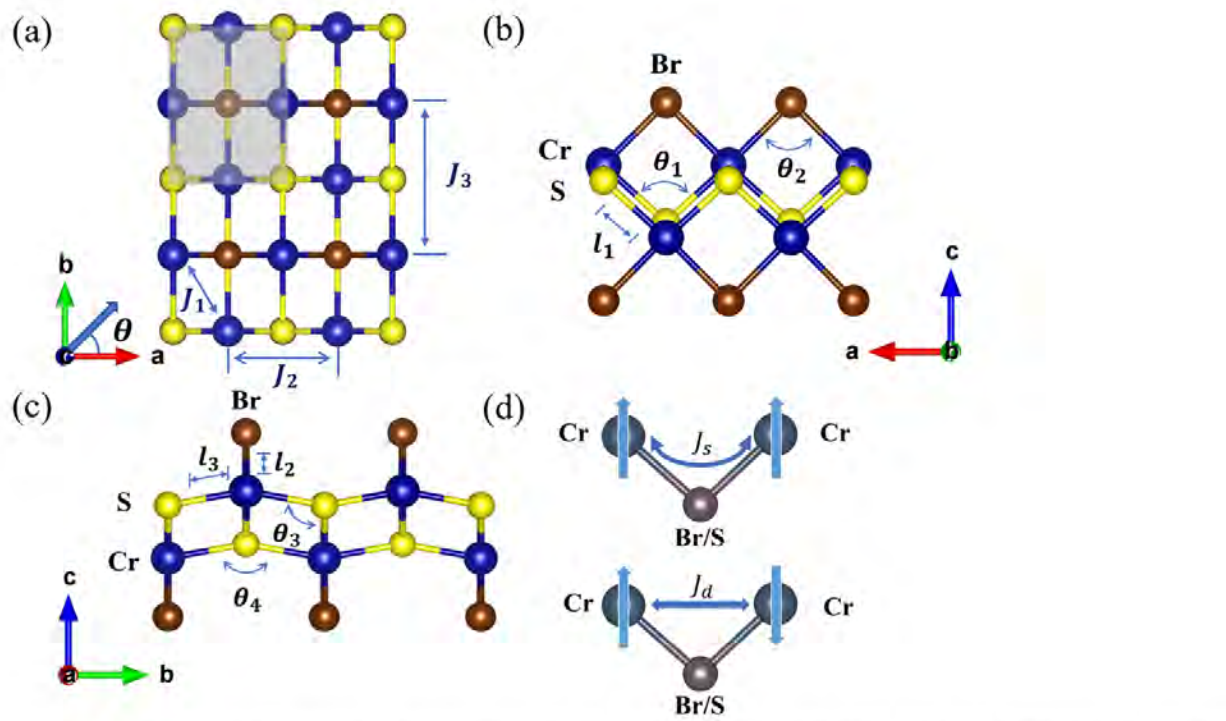

Fig. 1. Structure of monolayer CrSBr. (a) Top view, and the shaded part represents a unit cell, (b) and (c) different side views, where the distributions of atoms in three different directions are shown, and there are three different types of bond lengths l_i $(i = 1, 2, 3)$ and four different bond angles θ_i $(i = 1, ..., 4)$, respectively.

- A-type antiferromagnet
- T_N = 132 K in bulk
- Magnetic anisotropy is biaxial with easy axis along a-axis
- Interlayer exchange responds to strain along a-axis
  - Compressive – enhance AF
  - Tensile – reduce AF

Y. Diao et al.

Physica E: Low-dimensional Systems and Nanostructures 147 (2023) 115590

Strained CrSBr

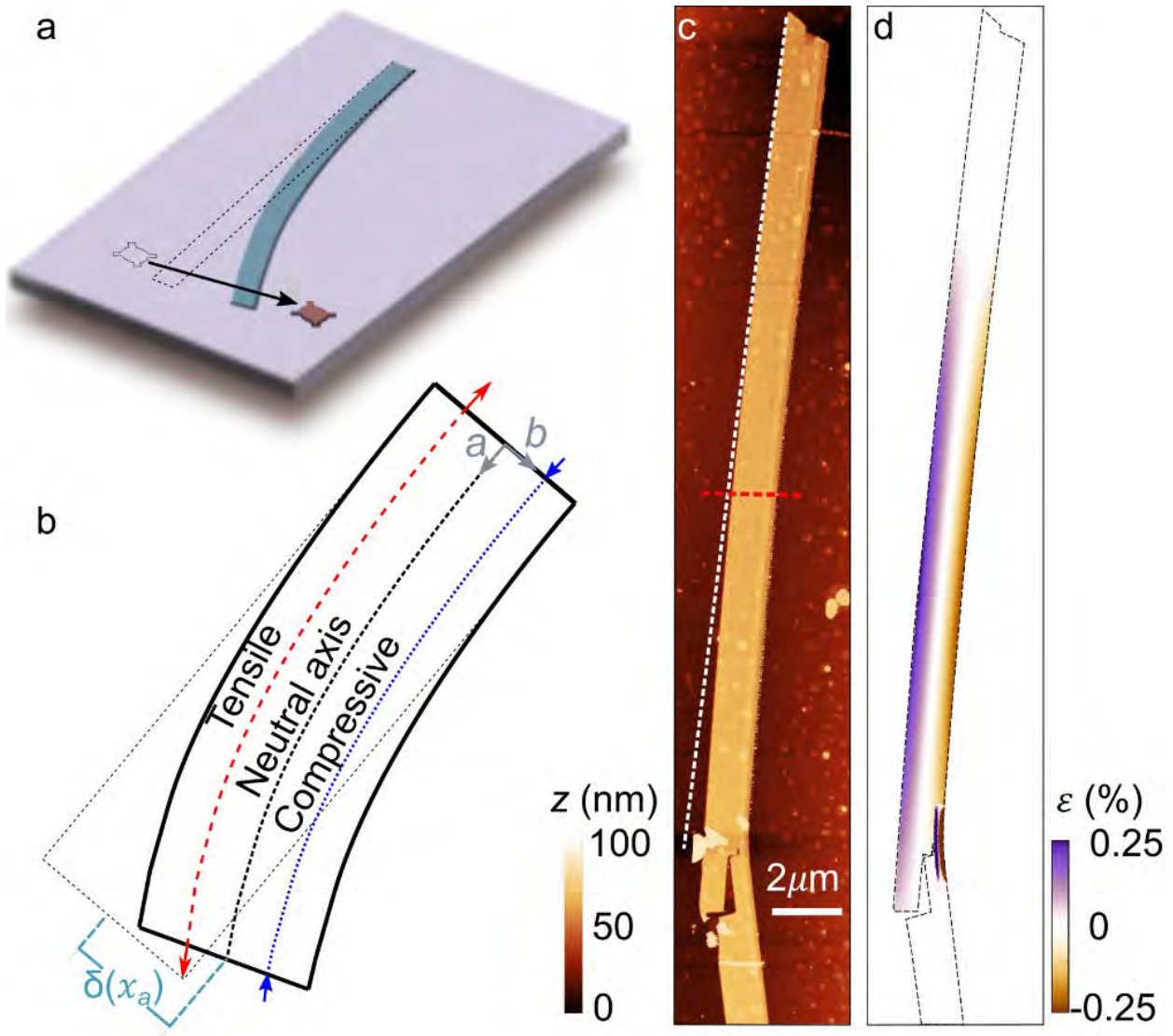

Bagani et al., *Nano Lett.* **24**, 13068 (2024).

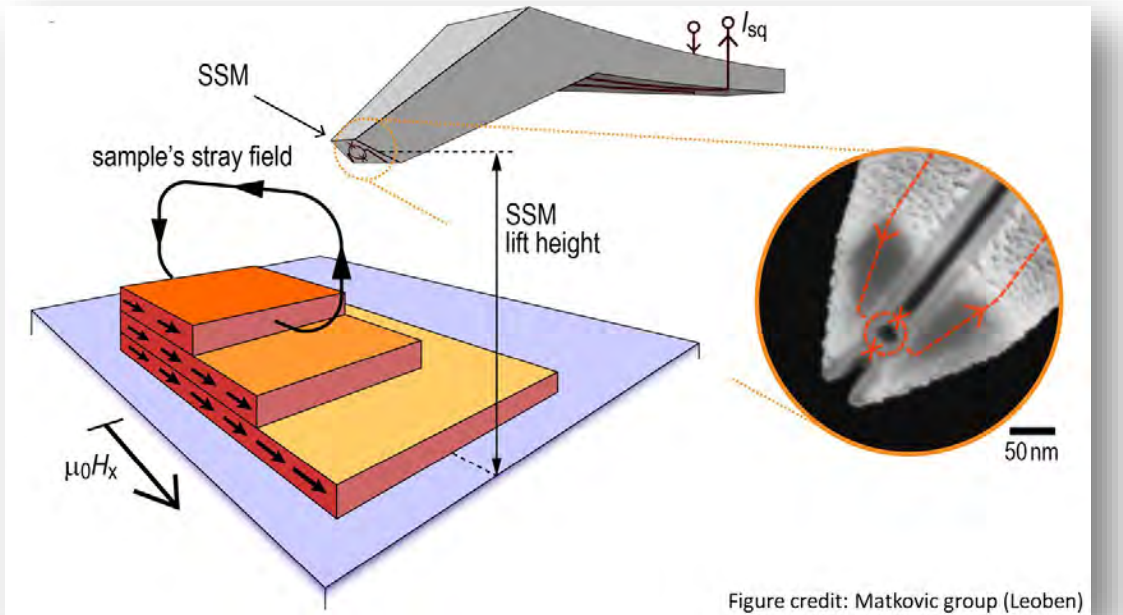

Figure credit: Matkovic group (Leoben)

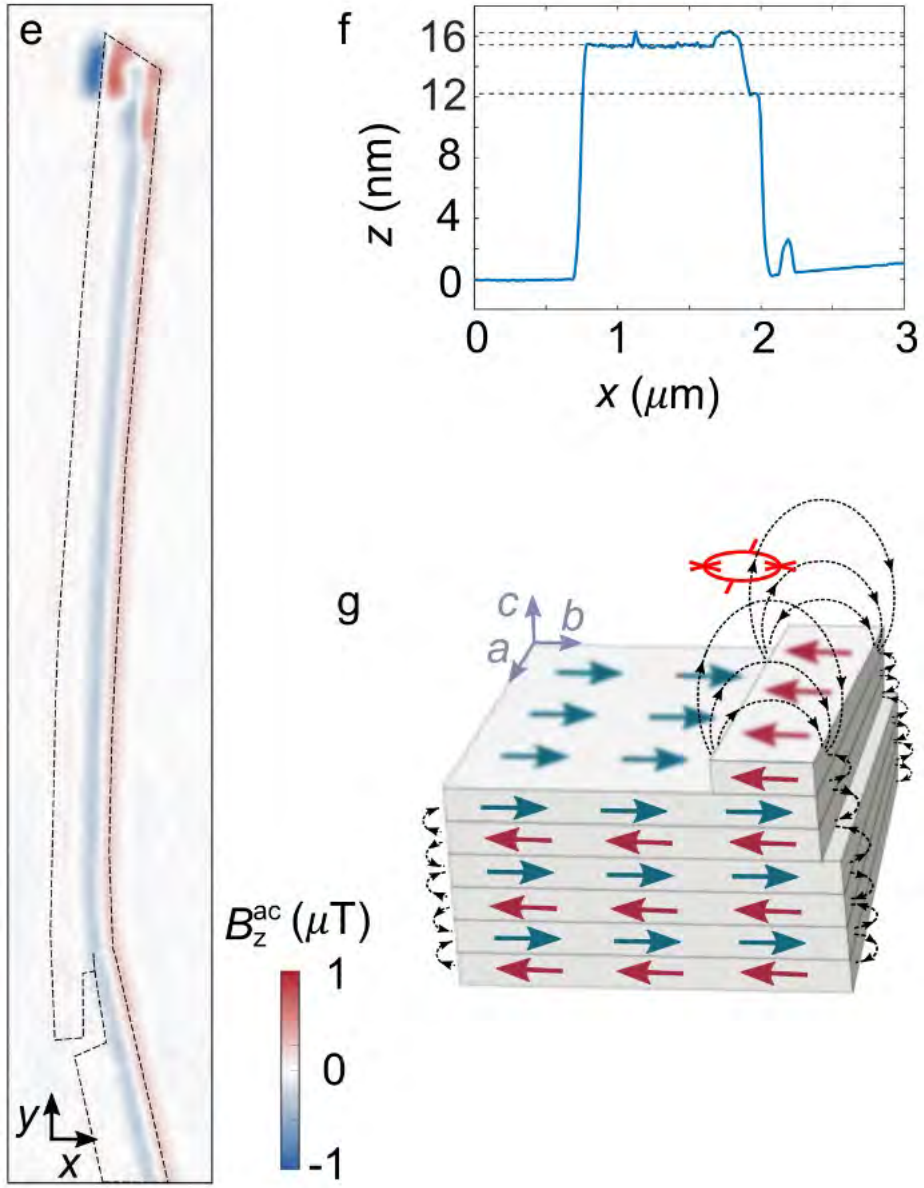

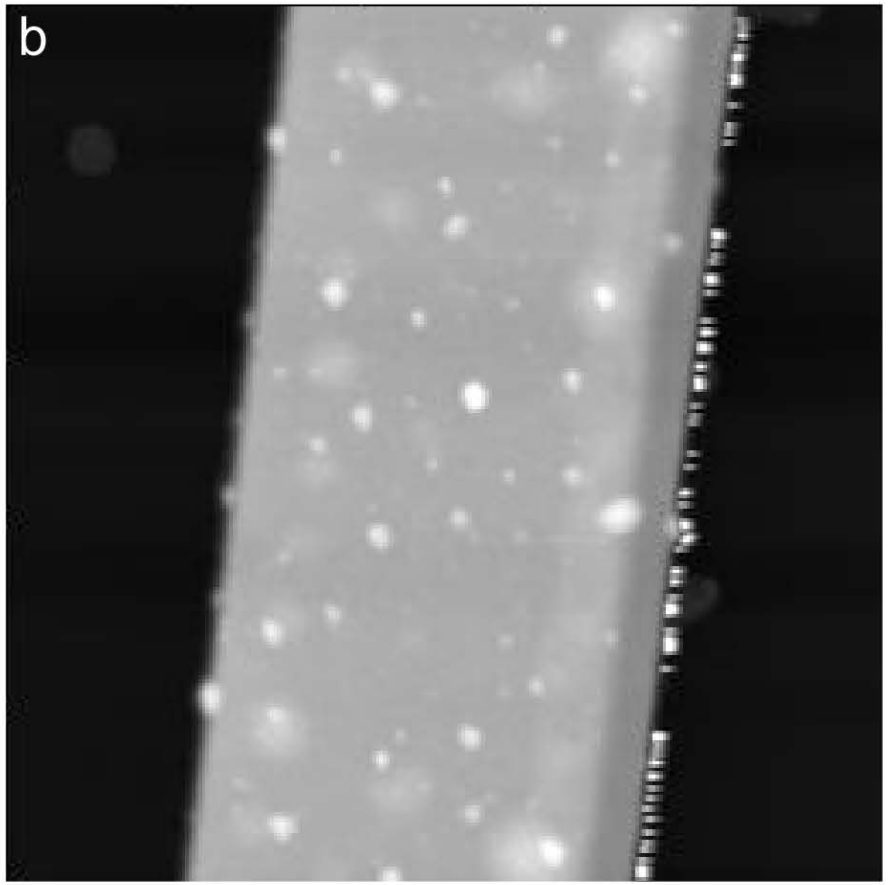

Bagani et al., *Nano Lett.* **24**, 13068 (2024).

Magnetic field dependence: strained sample

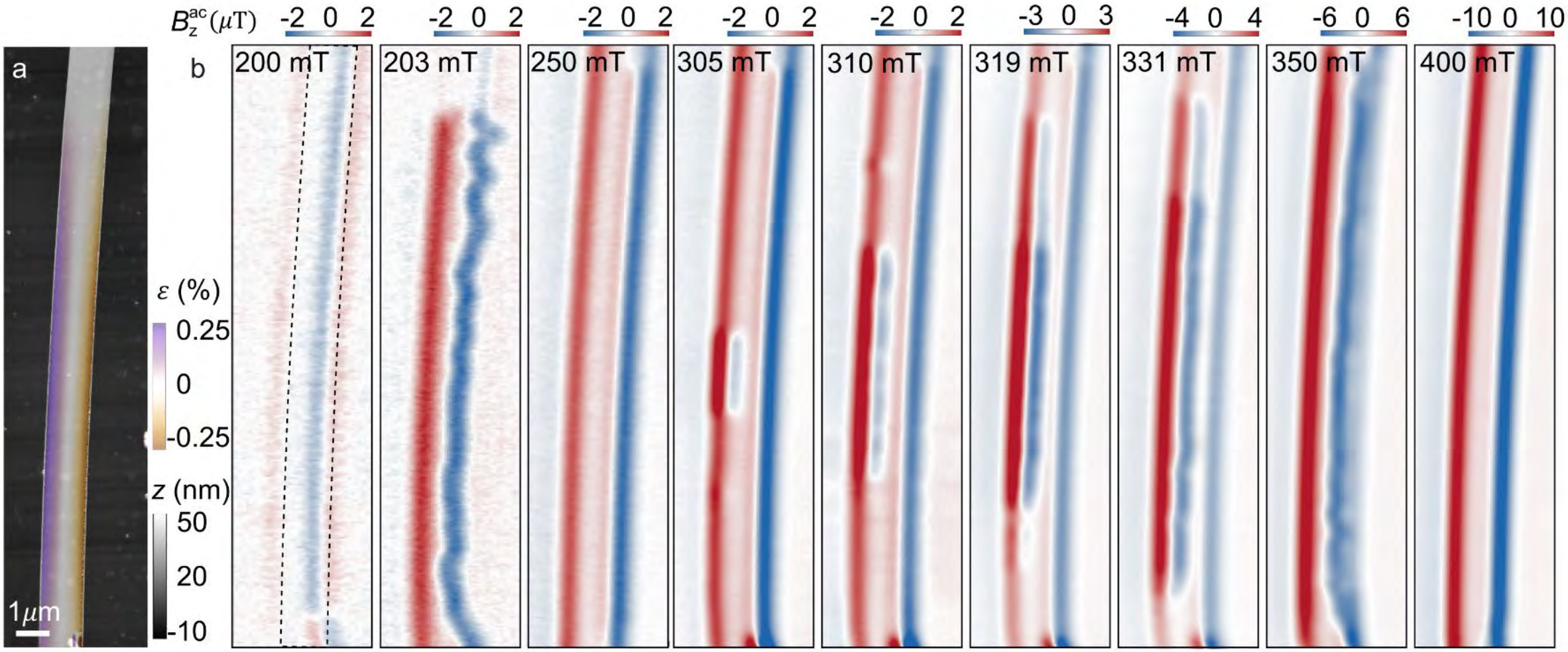

Bagani et al., *Nano Lett.* **24**, 13068 (2024).

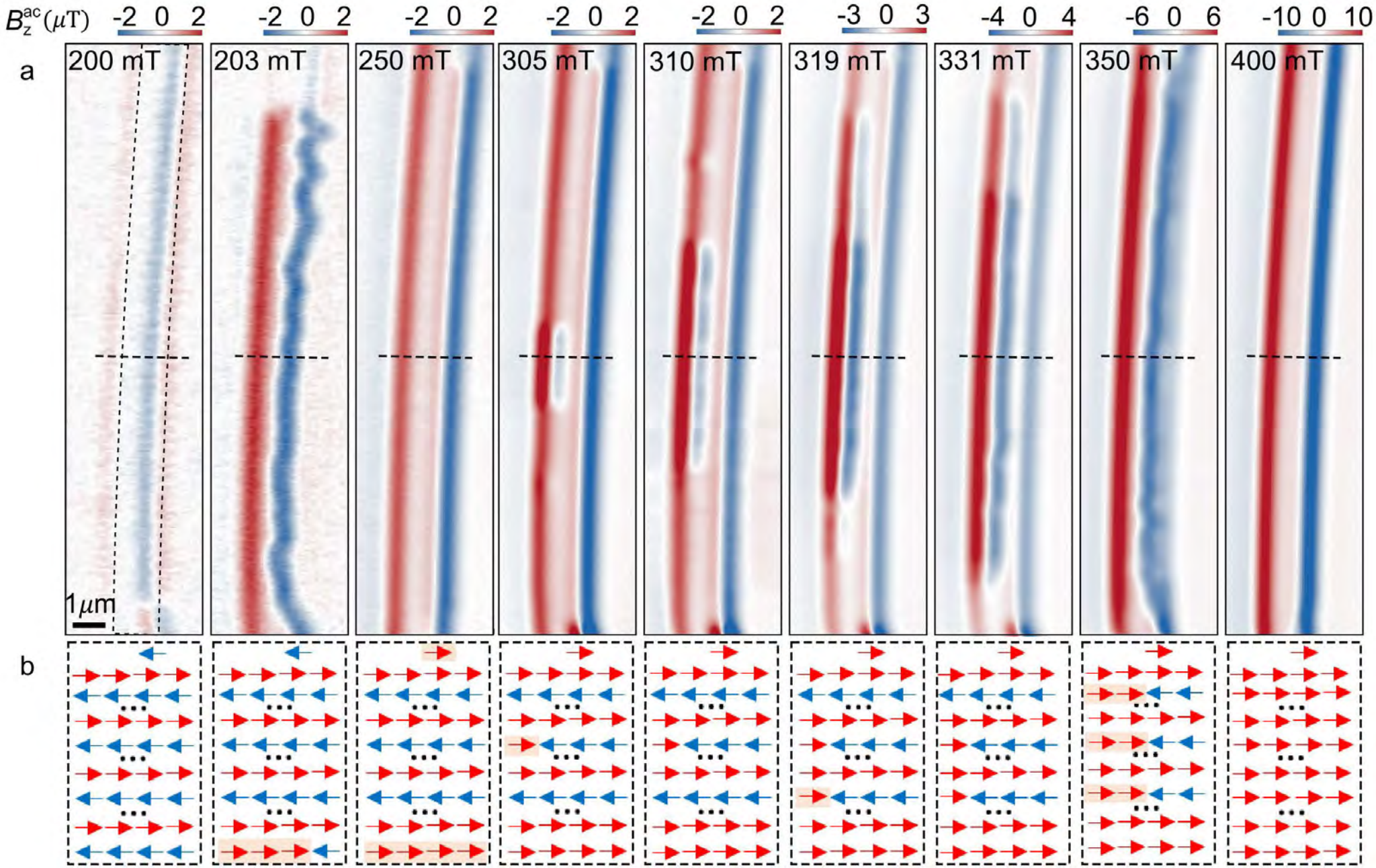

Bagani et al., *Nano Lett.* **24**, 13068 (2024).

Magnetic field dependence: pristine sample

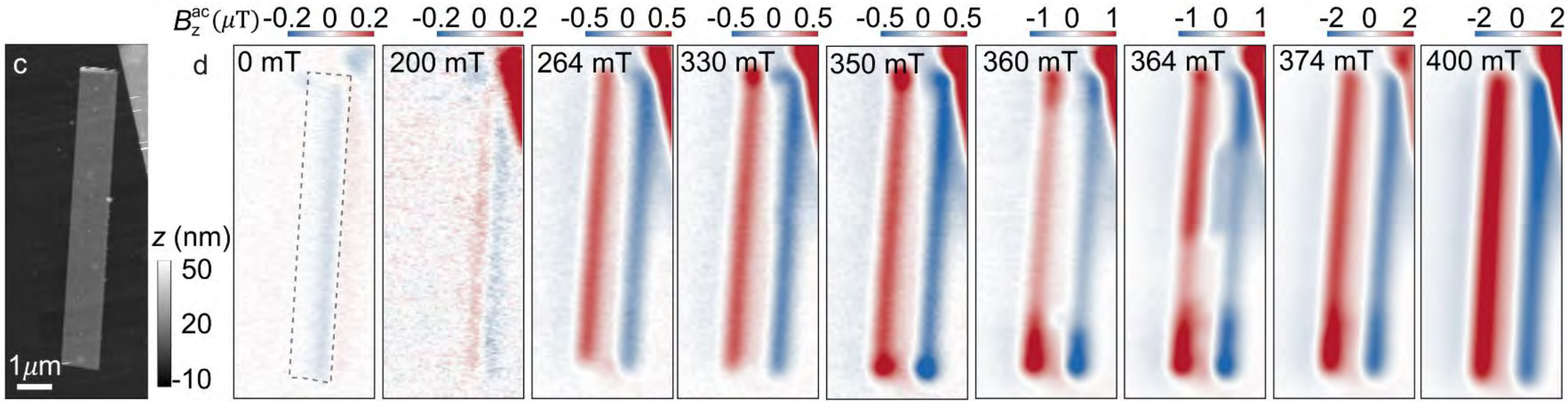

Bagani et al., *Nano Lett.* **24**, 13068 (2024).

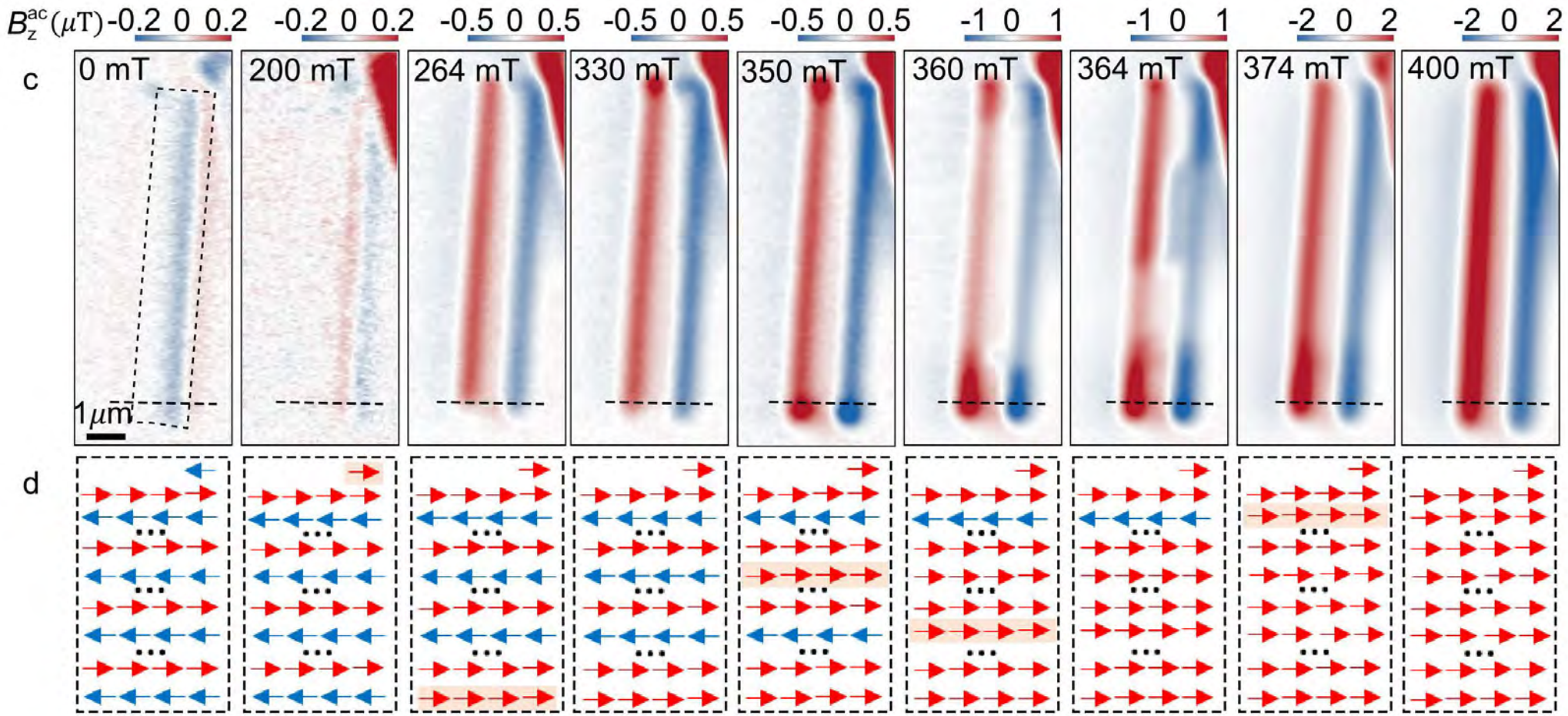

Bagani et al., *Nano Lett.* **24**, 13068 (2024).

Magnetic field dependence

Strained

Pristine

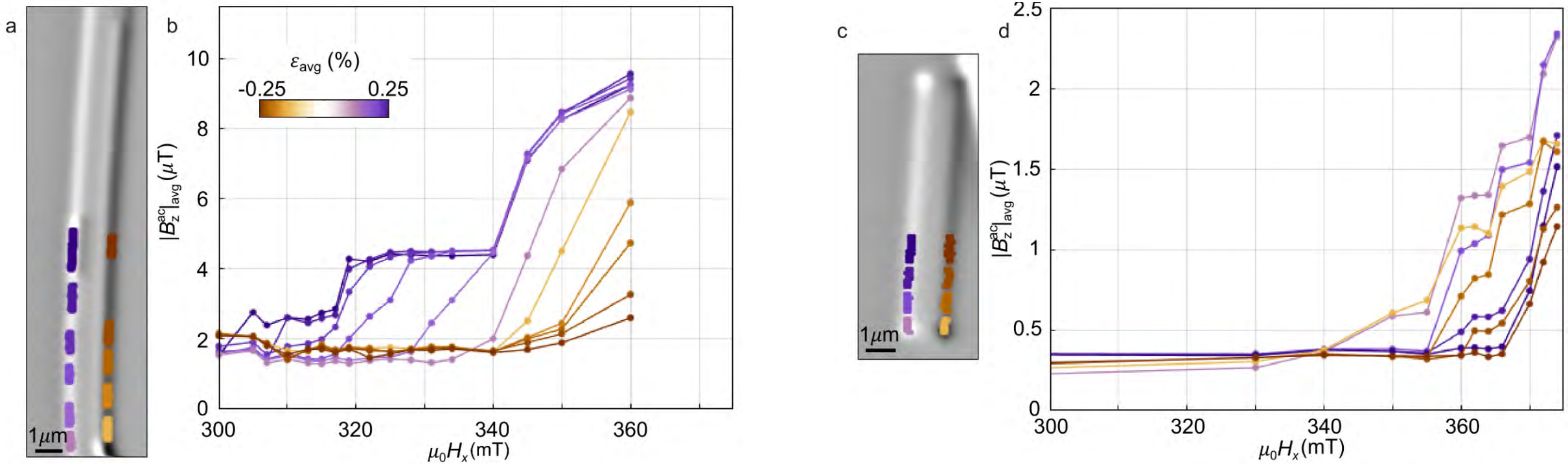

Bagani et al., *Nano Lett.* **24**, 13068 (2024).

Comparison to micromagnetic simulations

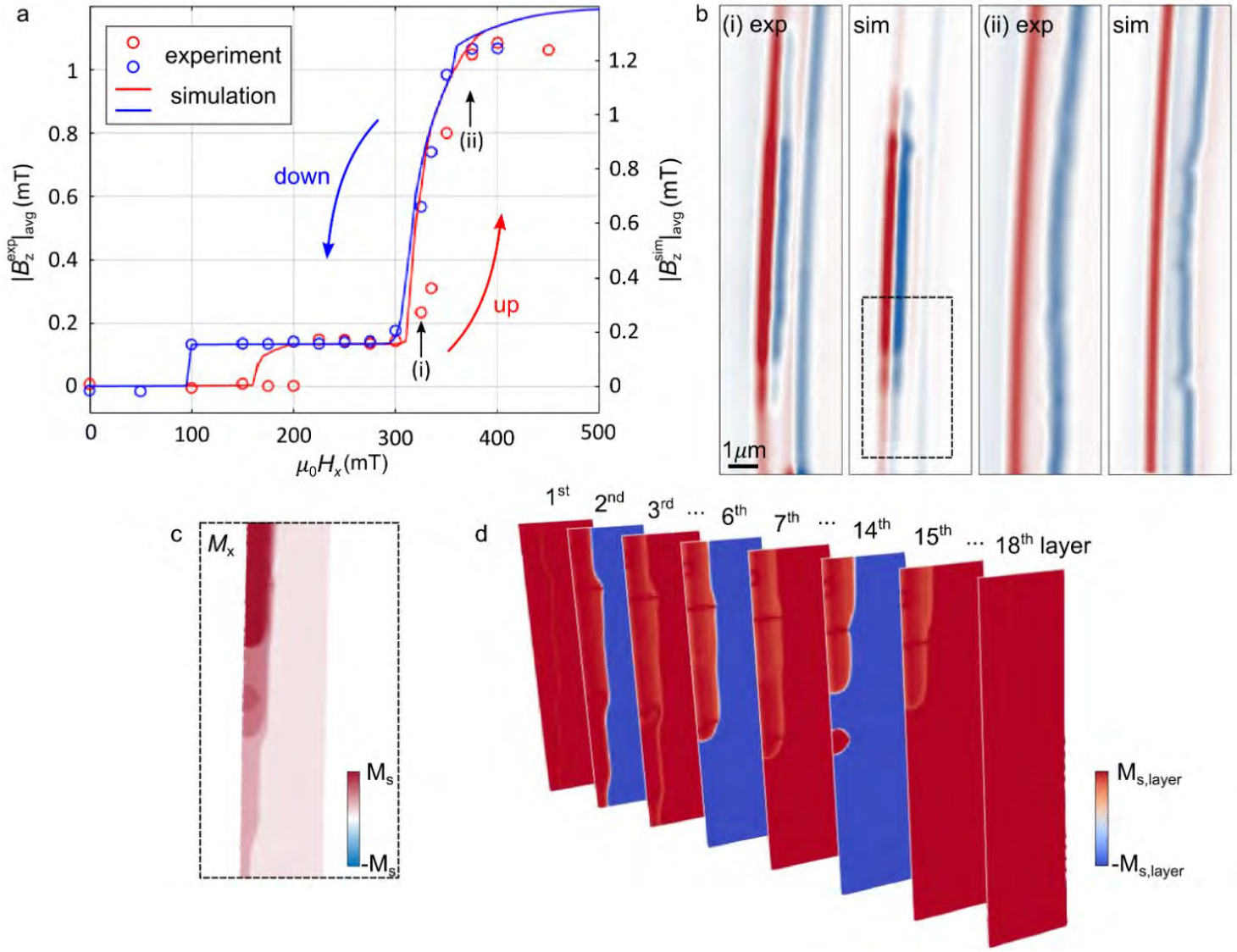

Bagani et al., *Nano Lett.* **24**, 13068 (2024).

Scanning SQUID microscopy of monolayer $CrPS_4$

Dr. Paritosh Karnatak

Research Scientist

Dr. Andriani Vervelaki

Post-doctoral Researcher

Katharina Kress

Ph.D. Student

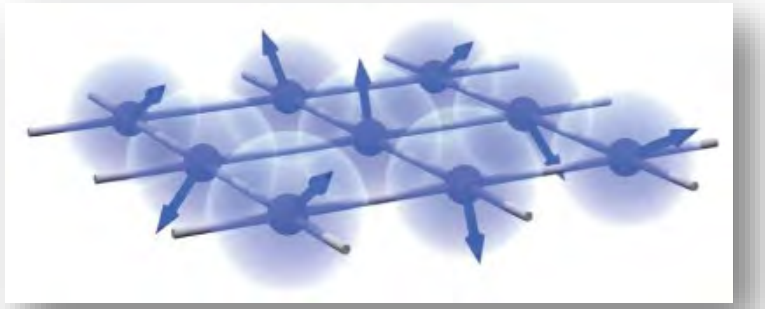

$CrPS_4$

- Bulk $CrPS_4$ is a van der Waals (vdW) A-type semiconducting antiferromagnet
- Weak out-of-plane anisotropy
- Neel temperature in bulk T_N = 38 K
- Monolayer's Curie temperature: T_C = 23 K

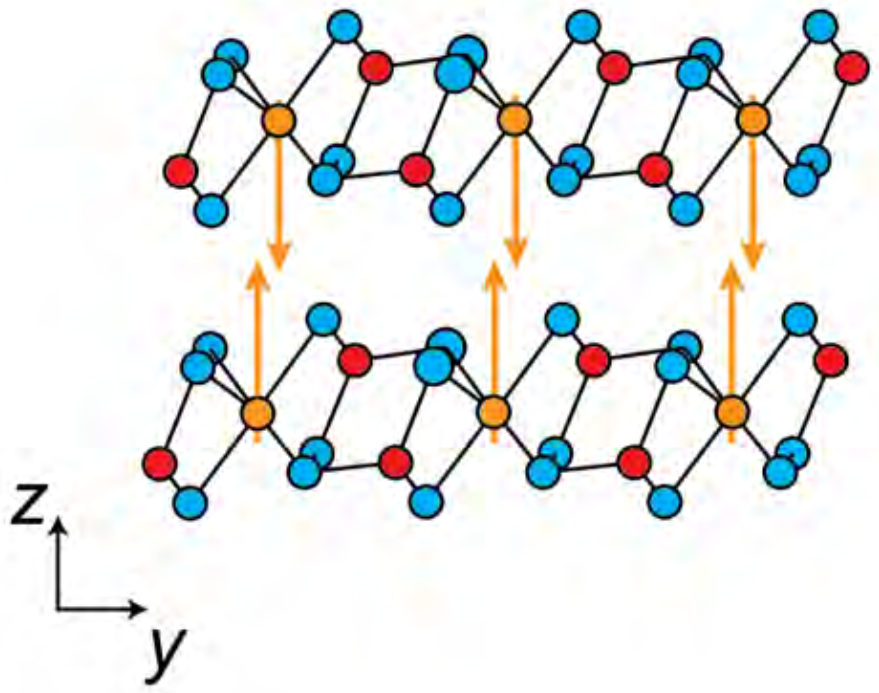

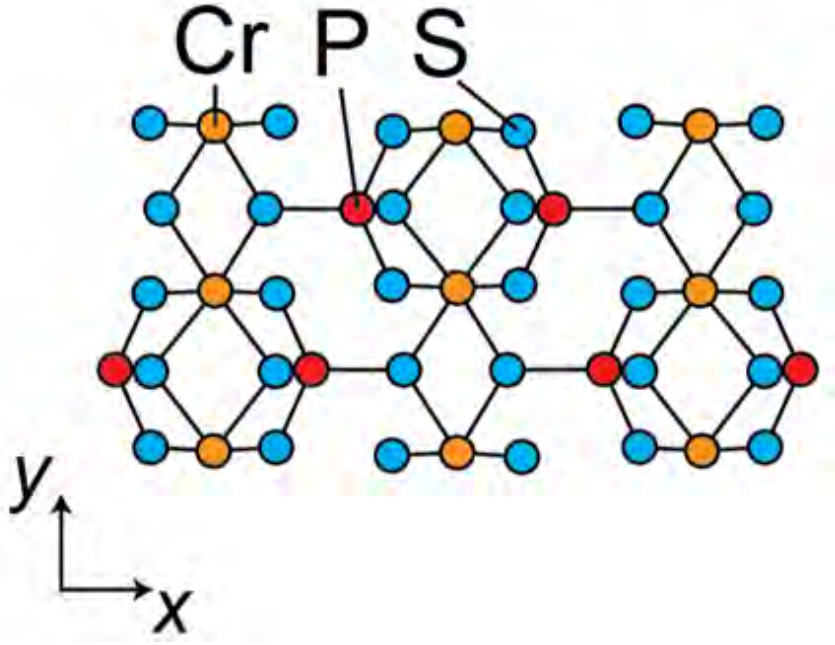

Collaboration with Morpurgo group, Geneva

$CrPS_4$

- Exfoliated $CrPS_4$ (CPS) with various thicknesses: 1 – 10s of layers
- CPS encapsulated with h-BN

Optical image before encapsulation

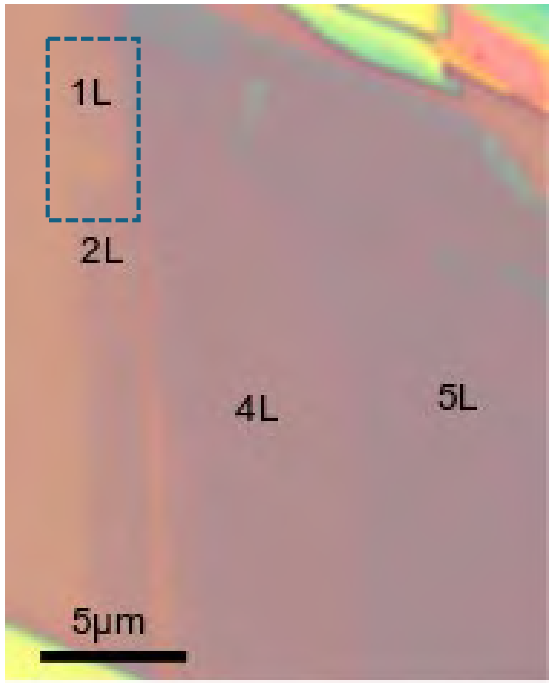

Fabrication:
Dr. Menghan Liao, Prof. Alberto F. Morpurgo
University of Geneva

Study: Imaging of the monolayer's (1L) magnetic reversal and comparison of the behavior with thicker areas

Stray field measurements

Optical image

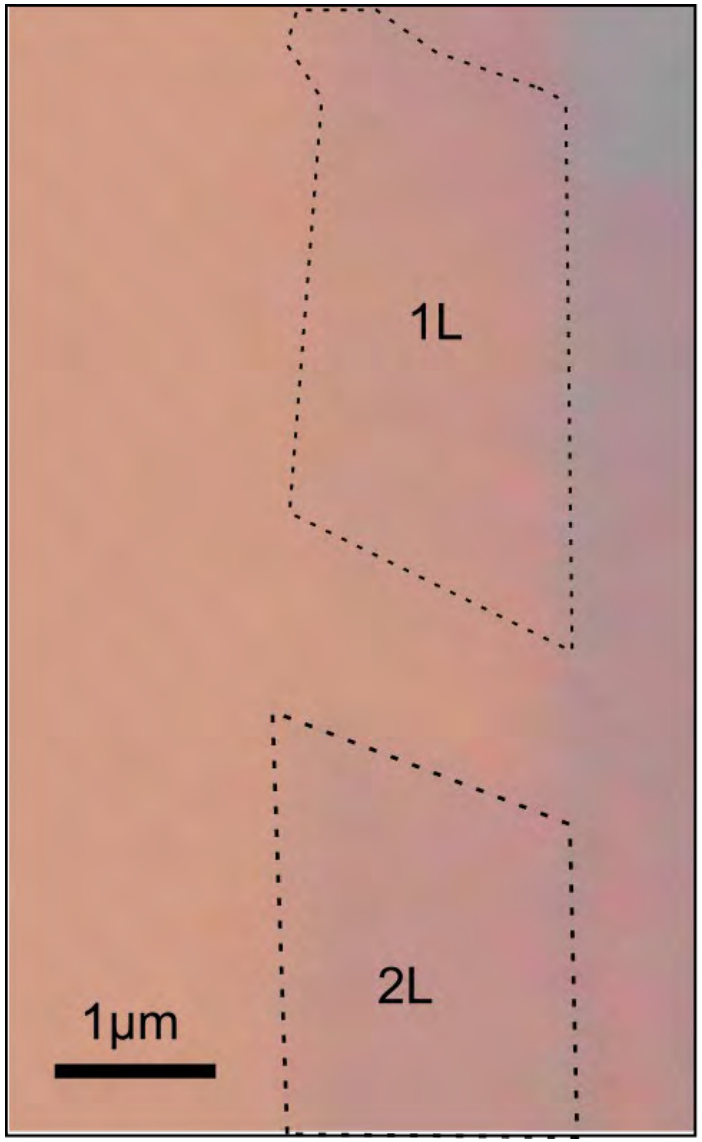

B_z^{ac} map

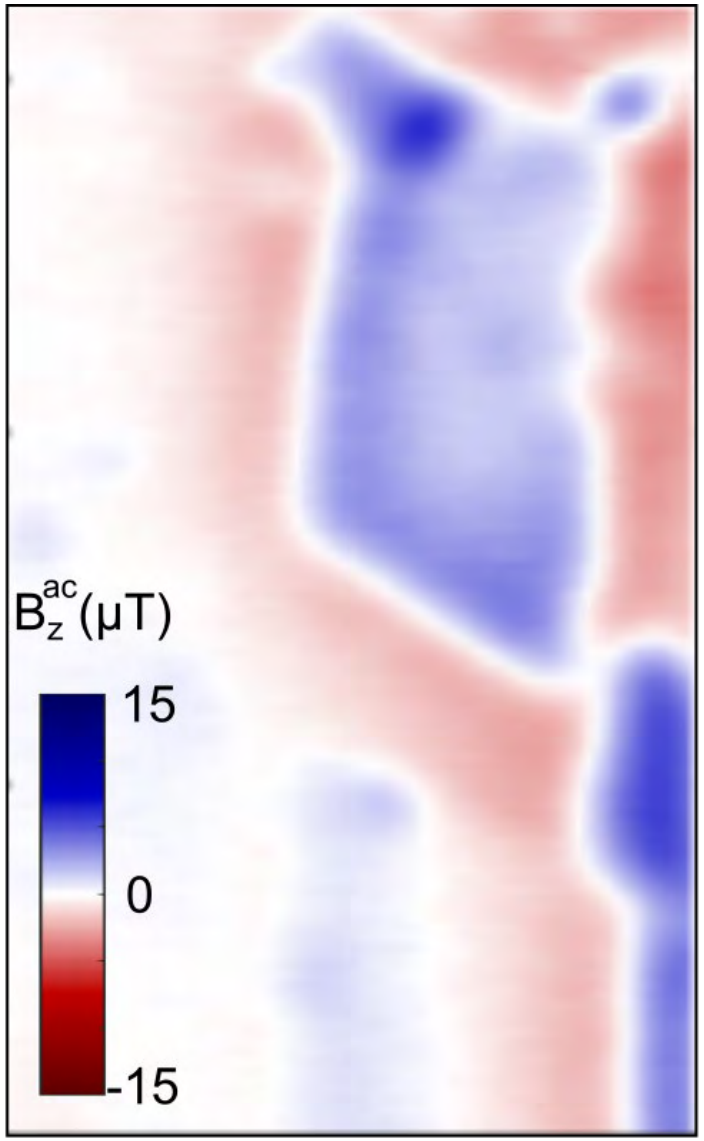

Magnetism in the monolayer

B_z^{ac} map

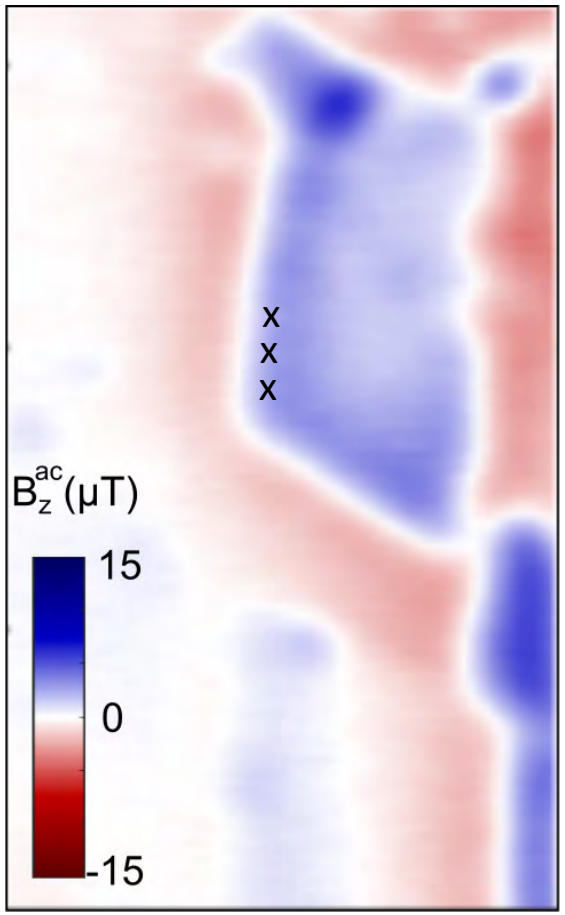

M_z map

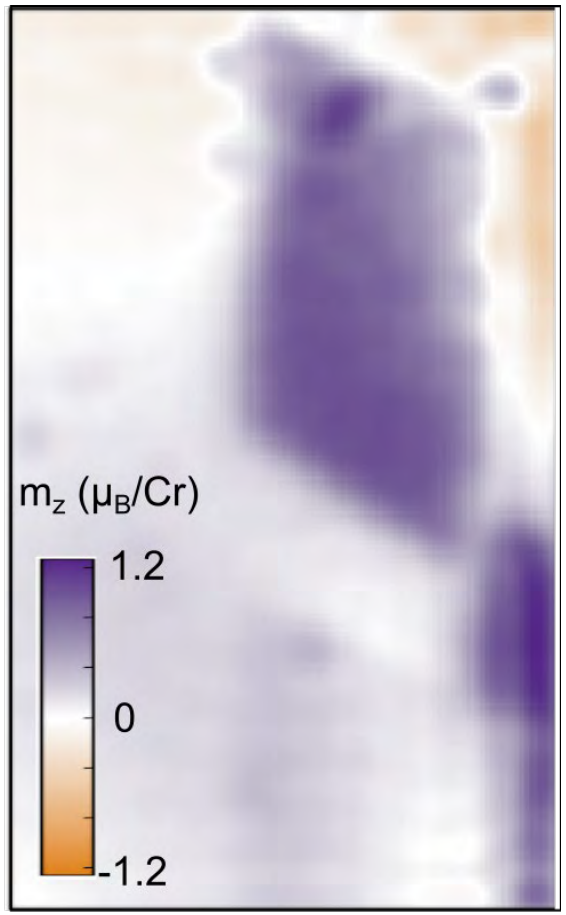

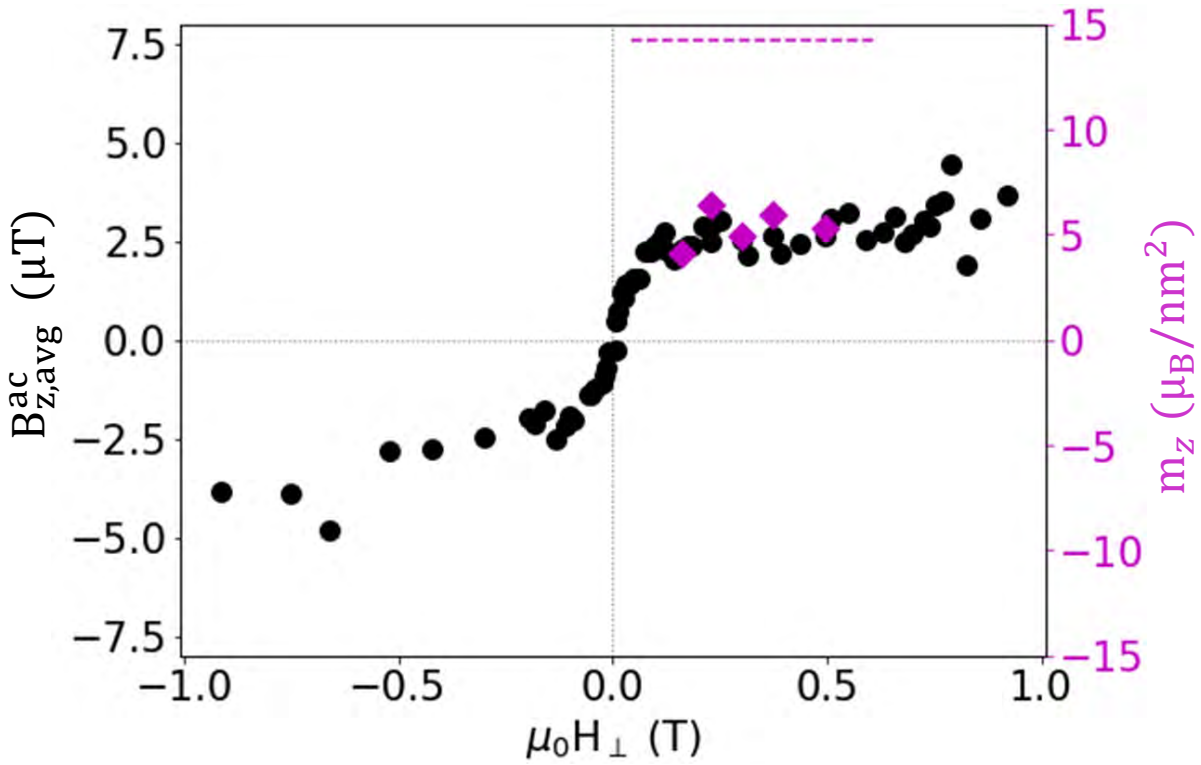

No remanence observed

At ~0.5 T, $\boldsymbol{m \leq 40\%}$ of the expected saturation magnetisation*

* Alcantara et al., *Phys. Rev. B*, 2023

Magnetisation reversal – few layers

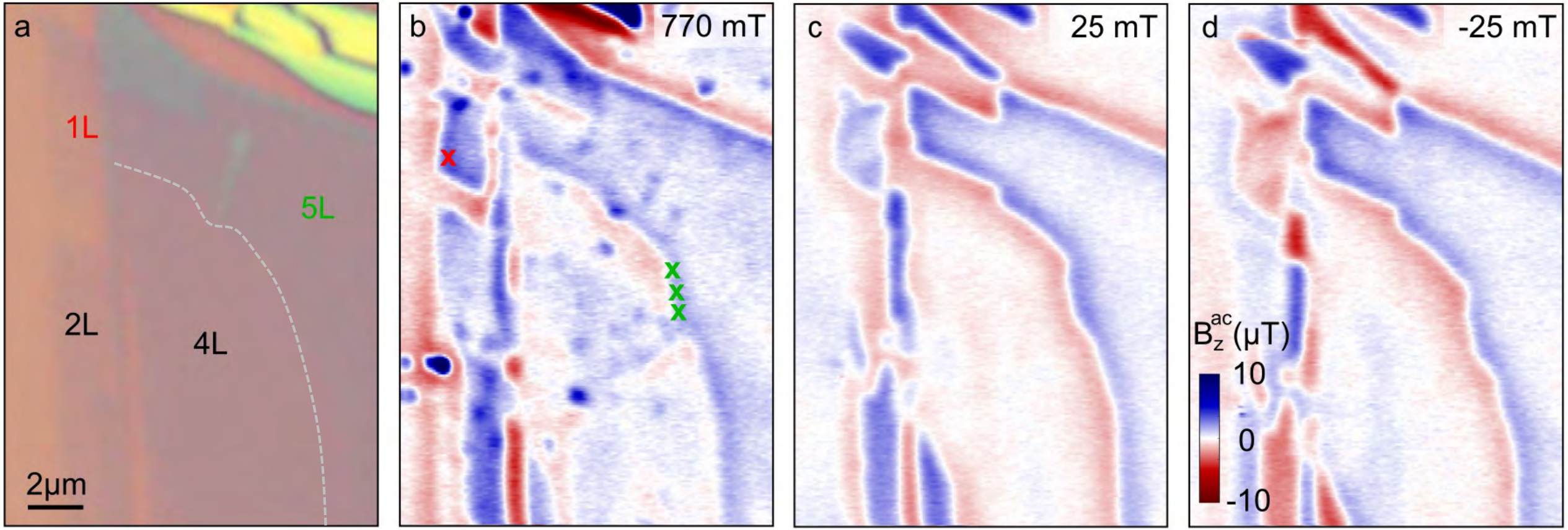

Magnetisation reversal – few layers

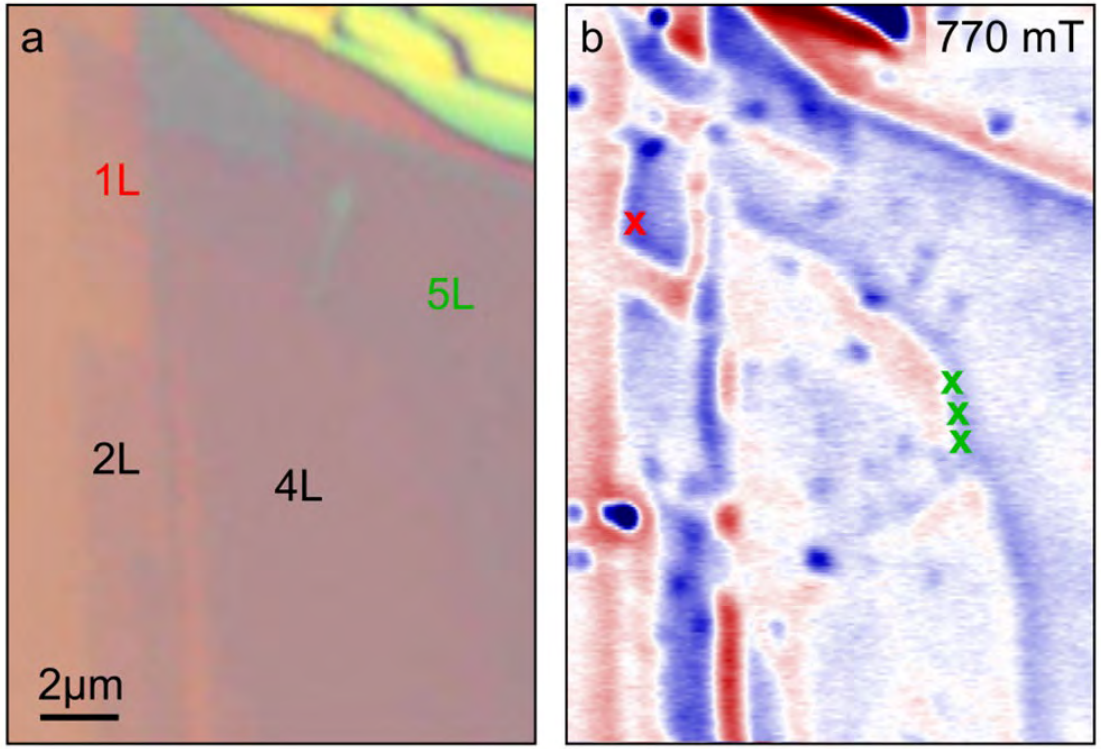

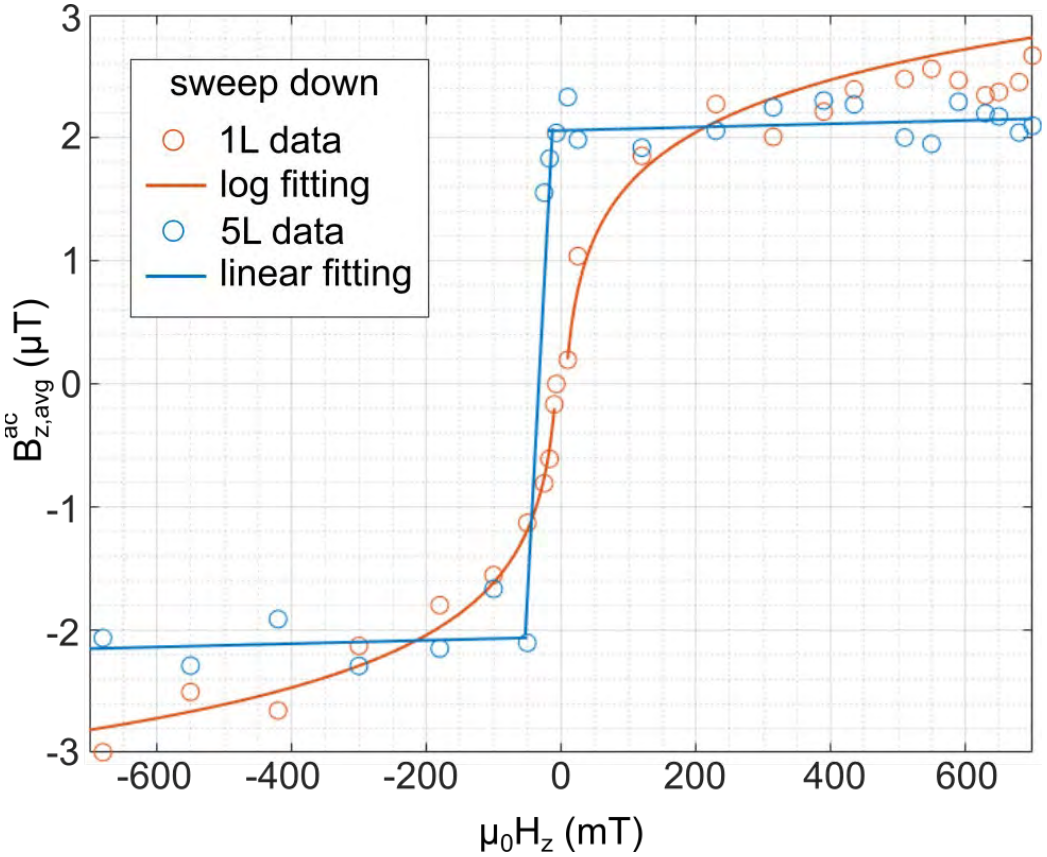

1L

- No retentivity
- Coercive field is ~ 0

5L

- $\sim 100\%$ retentivity
- 25 mT – 50 mT coercive field

Recent related references from our group

- **Reviews**
  - Magnetic microscopy for materials science: *J. Phys. Mater.* **7**, 032501 (2024)
  - Magnetic field imaging for 2D materials: *Nat. Rev. Phys.* **4**, 49 (2022)

- **Magnetic microscopy probes**
  - Nb and MoGe SQUID-on-tips: *Appl. Phys. Lett.* **122**, 192603 (2023)
  - SQUID-on-lever scanning probes: *Phys. Rev. Appl.* **17**, 034002 (2022)
  - Nanowire MFM fabricated by FEBID: *Phys. Rev. Appl.* **13**, 044043 (2020)

- **Chiral Magnets**
  - Imaging the surface of bulk Cu_2OSeO_3: *Commun. Mater.* **5**, 202 (2024)

- **2D Magnets**
  - Imaging 2D strained CrSBr: *Nano Lett.* **24**, 13068 (2024)
  - Imaging of 2D $Cr_2Ge_2Te_6$: *Commun. Mater.* **5**, 40 (2024)
  - MFM of bilayer $EuGe_2$: *Nanoscale* **16**, 5302 (2024)